Electronic Supplementary Information for

Mn-based Molecular Catalysts for the Electrocatalytic Disproportionation of CO_2 into CO and CO_3^{2-}

Tessa H. T. Myren, [†§] Abdulaziz Alherz, [‡§] Jonathan R. Thurston, [‡] Taylor A. Stinson, [†]

Chloe G. Huntzinger, [†] Charles B. Musgrave, [‡*] Oana R. Luca[†*]

[†]*Department of Chemistry and* [‡]*Department of Chemical and Biological Engineering,*

University of Colorado Boulder, Boulder CO, 80300 USA

Fax: (+)1 303 739 6721

*E-mail: charles.musgrave@colorado.edu, oana.luca@colorado.edu

[§]*equal contributors*

Table of Contents

1. General Methods

General methods. Except where noted, reactants were used as received from commercial sources without further purification. Synthesis of the ligands and the metallated complex were synthesized as previously reported.[1] Tetrabutylammonium hexafluorophosphate (TBAH) was recrystallized from ethanol then dried under high vacuum for 24 hours before use. Metal complexes were stored in low-light conditions to prevent light exposure and degradation. All NMR spectra were gathered on a Bruker Avance-III 300 MHz NMR Spectrometer at room temperature with chemical shifts reported with respect to internal proton or carbon solvent for ^{1}H and ^{13}C NMR spectra, respectively. A Nicolet iS5 FTIR Spectrometer was used to collect infrared spectra using a KBr card.

2. Electrochemical Experiments

A standard three electrode setup with a glassy carbon working electrode (3mm, Bioanalytical Systems), a platinum wire counter electrode, and a silver wire single junction pseudo-reference were used for Cyclic Voltammograms (CVs) and Normal Pulse Voltammograms (NPV). For electrolysis experiments a carbon cloth counter electrode was used in place of the platinum wire. Ferrocene was used an external standard. All experiments were done with a rigorous exclusion of air using an argon purge. In the case of NPVs, concentrations were adjusted for evaporated solvent in order to calculate the number of electrons accurately. All data workup was done via OriginPro vb9.4.0.220 software.

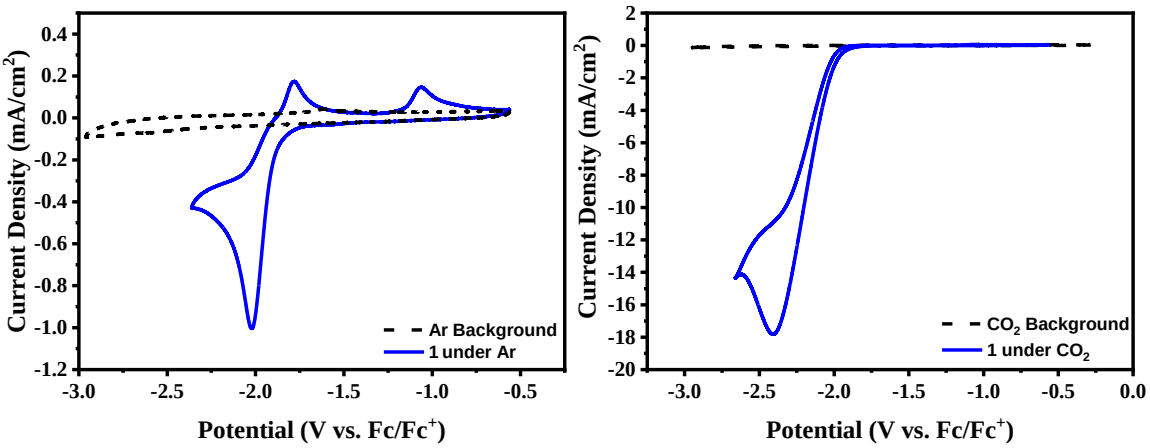

Figure S1. (Left) Cyclic voltammogram of **1** ($MnCNC^{Bn}$) in blue. The black dashed line is the background taken under argon. (Right) CV of **1** in blue under CO_2 in the absence of a proton source with a background under CO_2 shown in black.

Table S1. Relative rates of product formation during CO_2 reduction electrocatalysis with 0.28 M concentration for $[CO_2]$ in MeCN.

$[CO_2]_0$	Fraction %	Relative Rate 1	Relative Rate 2	Average	Stdev
0.028	0.1	1	1	1	0
0.056	0.2	4.291667	3.892857	4.092262	0.282001
0.084	0.3	5.708333	5.214286	5.46131	0.349344
0.168	0.6	8	7.089286	7.544643	0.643972

3. Infrared Spectroscopy

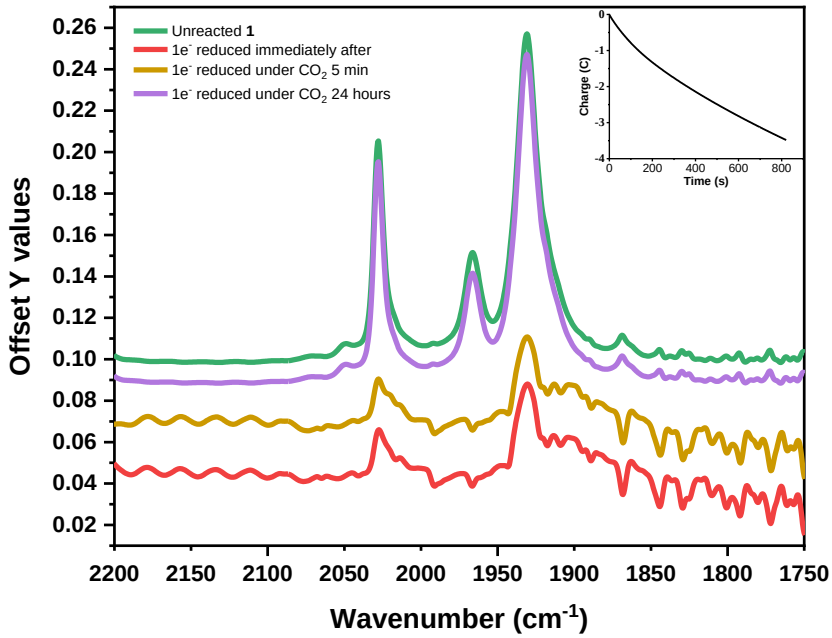

Figure S2. IR Spectra collected during of a series of experiments using **1**, showing the peaks in the region of carbonyl stretches.[2] Green shows the spectrum of unreacted **1**, red is **1** after a one electron electrochemical reduction under argon, yellow is the solution from that reaction after being placed under CO_2 for 5 min and purple is under CO_2 for 24 hours. (Inset) The charge vs. time plot of the one electron electrochemical reduction of **1** under argon. Precipitation only occurs after the samples are left standing but is not observed during the experiment.

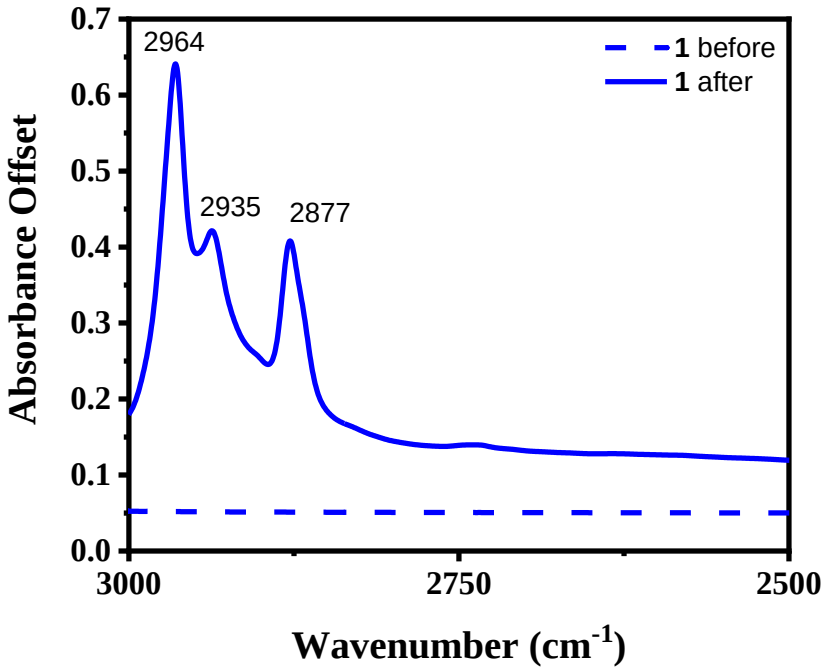

Figure S3. IR Spectra before and after electrolysis in the 2500 to 3000 cm^{-1} range Comparison of **1** before and after electrolysis under CO_2. The dashed and solid blue lines are **1** before and **1** after, respectively. The peaks at 2964 cm^{-1} and 2935 cm^{-1} correlate with the presence of a carbonate species in solution.

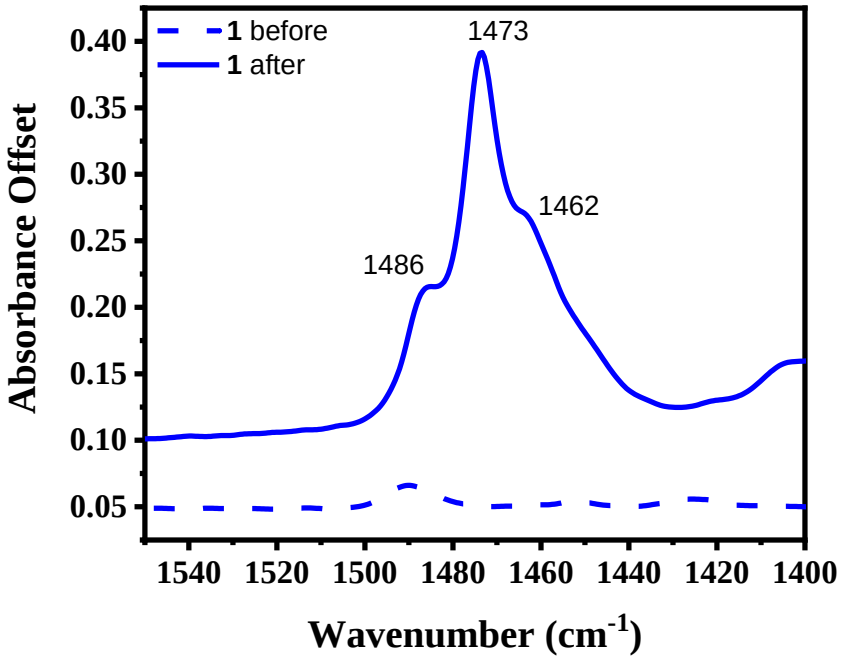

Figure S4. IR Spectra before and after electrolysis in the 1400 to 1600 cm^{-1} range. Similar to Figure S3, the peaks at 1473 cm^{-1} indicate the presence of carbonate after electrolysis under CO_2 in **1**. Dashed line: before electrolysis and solid line: after.

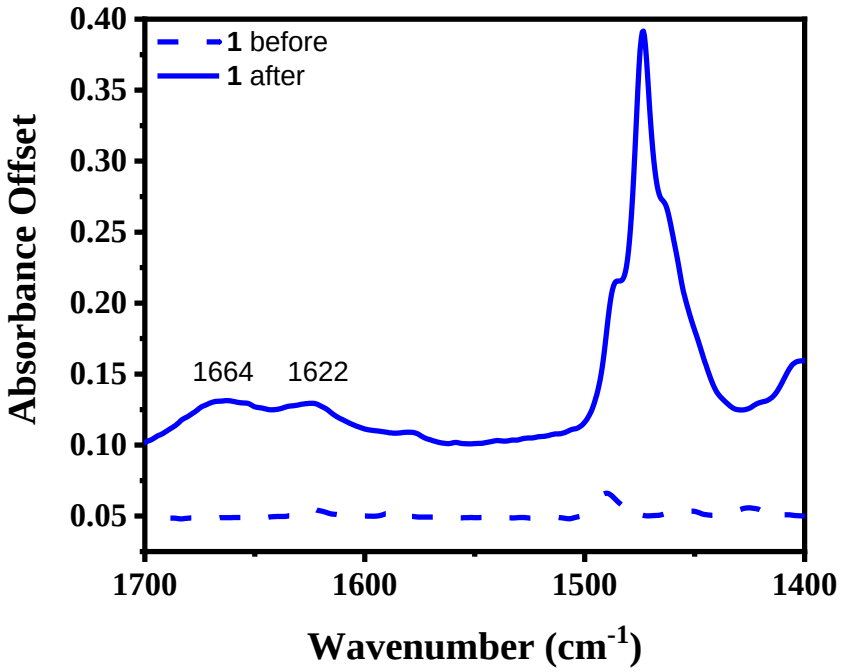

Figure S5. IR Spectra before and after electrolysis in the 1400 to 1700 cm^{-1} range. The peaks at 1664 and 1622 cm^{-1} are present in the region indicative of carbonate formation after electrolysis under CO_2.[2-3] Blue is **1** with dashed lines indicating before electrolysis and solid lines after.

4. Quantification of Carbonate using GC-EI

The derivatization method for the quantification of carbonate was performed akin to literature precedent. (https://pubs.acs.org/doi/full/10.1021/ac1007688) Standard solutions of CO_3^{2-} for calibration were prepared using sodium carbonate in water. For quantification, analyte solutions from electrolysis were dried via rotary evaporation followed by high vacuum then dissolved in 20 mL of HPLC grade water to maintain the original concentration following electrolysis. For derivatization 100 µL of solution was mixed with 800 µL deuterated acetone (CD_3COCD_3) and 20 µL of 2,3,4,5,6-pentafluorobenzyl bromide. This mixture was then heated to 50°C for 60 minutes in an aluminum heating block. Acetone was then removed from the solution under a stream of argon and toluene was used to extract the reaction products. A portion of the toluene aliquot was then diluted 1:50 for the GC-MS injection.

Data was collected on a Thermo ISQ LT GC-MS in EI mode with an electron energy of 70 eV. The column used was a Zebron ZB-5HT [30 m x 0.25 mm inside diameter, 0.25 µm film thickness]. Samples were collected in split mode with a column flow of 1 mL/min, purge flow of 10 mL/min, and a split flow of 10 mL/min. Inlet and ion source temperature were held at 200°C and 180°C respectively. Aliquots (1 µL) of the 1:50 dilution from the derivatization procedure were injected. The oven starting temperature was 120°C held for 1 min followed by a ramp of 60°C/min up to 300°C which was held for 9 minutes. Quantitative analysis was performed by extracting the ion for *m/z* 418.

5. Determination of Kinetic Order in Catalyst Using the Normalized Timescale Method and Voltammetry

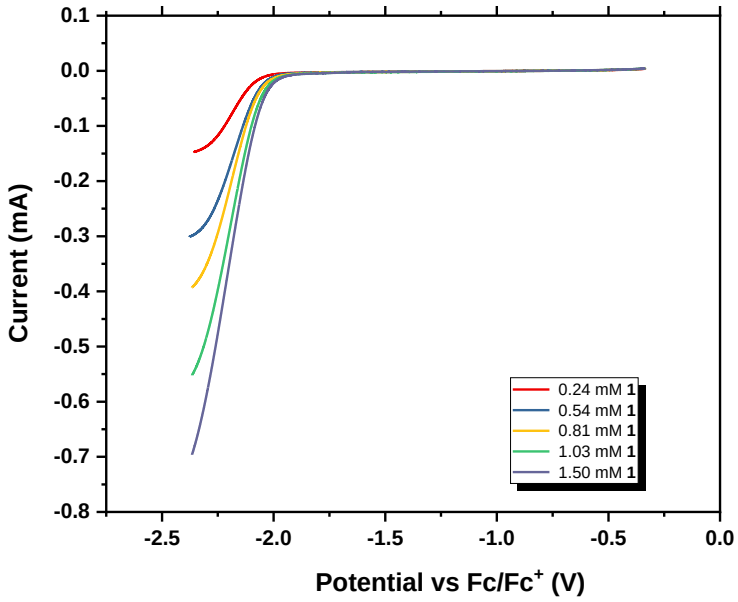

Figure S6. Reductive voltammogram scans of the catalytic conditions were collected at concentrations of 0.24 mM, 0.54 mM, 0.81 mM, 1.03 mM and 1.5 mM catalyst at CO_2 saturation.

Plots of charge passed vs time were then generated for each of the runs using EC-Lab and the x-axis was multiplied by the concentration of catalyst raised to the power of the kinetic orders of 0.5, 1 and 2 to identify overlay.

6. Computational

Computational Details

Density Functional Theory calculations were performed in Gaussian 16[4-5] based on the MN15 density functional.[4-5] The Stuttgart/Dresden SDD basis set/pseudopotentials[6] was used to describe Mn atoms and the double-zeta 6-31+G(d,p) basis set[7] was used to describe all other atoms. Vibrational force constants at this level of theory were calculated to (a) validate that all geometries have only positive vibrational frequencies and (b) to compute entropies, zero-point energies, and thermal corrections for the reported free energies at 298 K. An implicit polarized continuum solvation model (CPCM) was used to simulate the solvation effects of acetonitrile.[8-9] All charge and spin densities were projected using natural-bond orbitals (NBO).[10]

Reduction Potential Calculations:

Reduction potentials E^0 versus the ferrocene electrode (vs. Fc/Fc^+) in acetonitrile were calculated using the aforementioned levels of theory according to the following equation[11]:

$$\Delta G_{red} = G_{RH} - G_{RH^+} \quad (1)$$

$$E^0 = -27.2114\ \Delta G_{red} - 4.988\ V \quad (2)$$

This was checked against experimental results and found to be in agreement within 0.3 V.

Acidity Calculations:

pK_a values are calculated according to the following equation, following the works of Schlegel[12]:

$$pK_a = \frac{\Delta G}{2.303RT} \quad (3)$$

$$\Delta G = G_{A^-} - G_{AH} + G_{H^+} \quad (4)$$

A G_{H^+} value of -248.225 kcal/mol is used. This value has been determined by a scaling approach using multiple acids with experimentally determined pKa values to extrapolate GH+. The set of acids used to determine G_{H^+} is obtained from REF [13].

Mechanism A Charge Densities

Charge densities of intermediates participating in the proposed Mechanism A, as projected by NBO Natural Bonding Orbitals.

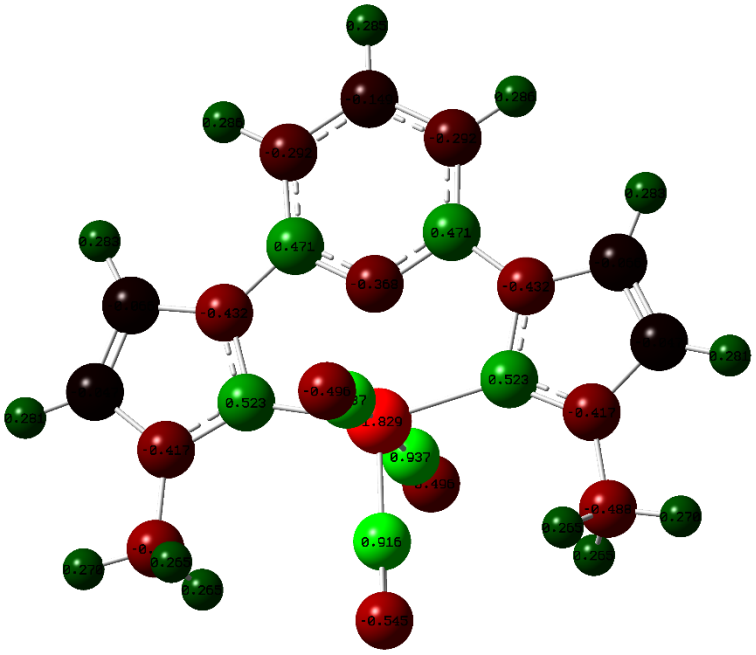

Figure S7. Charge density of **I**.

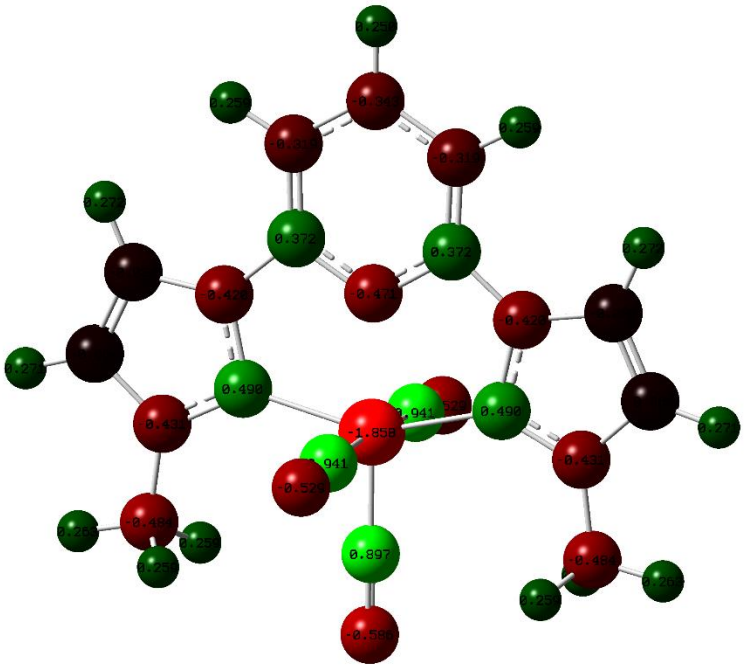

Figure S8. Charge density of **II**.

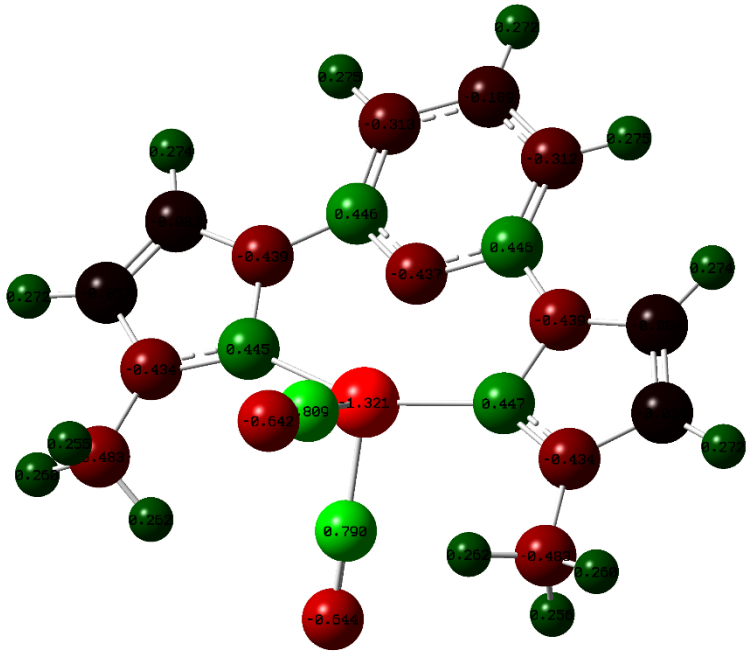

Figure S9. Charge density of **III**.

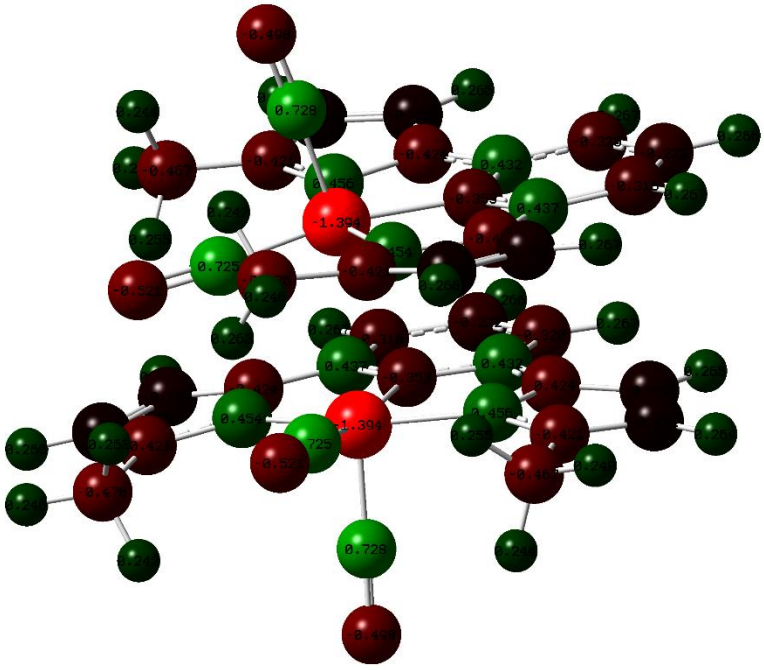

Figure S10. Charge density of **III** Dimer.

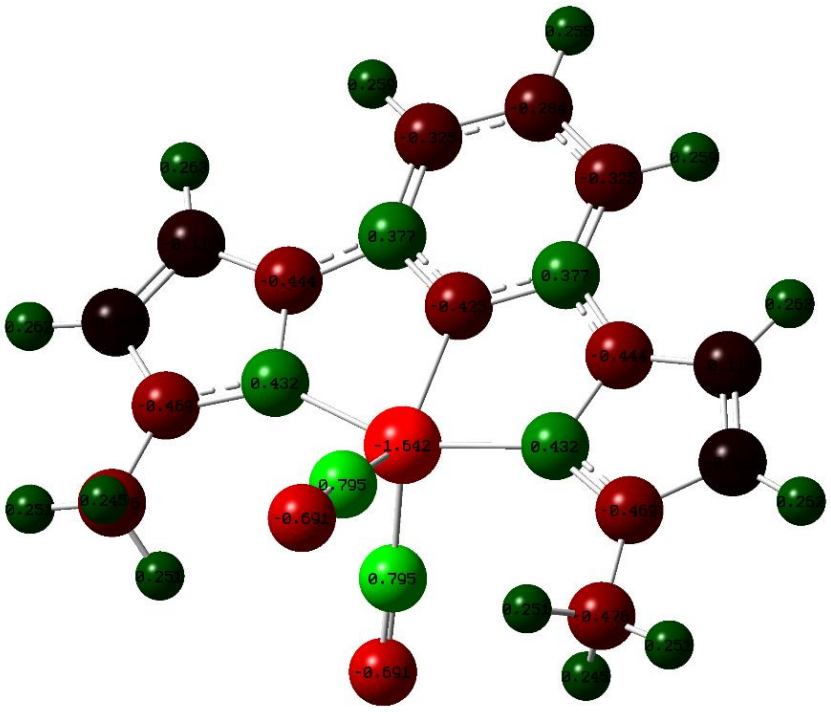

Figure S11. Charge density of **V**.

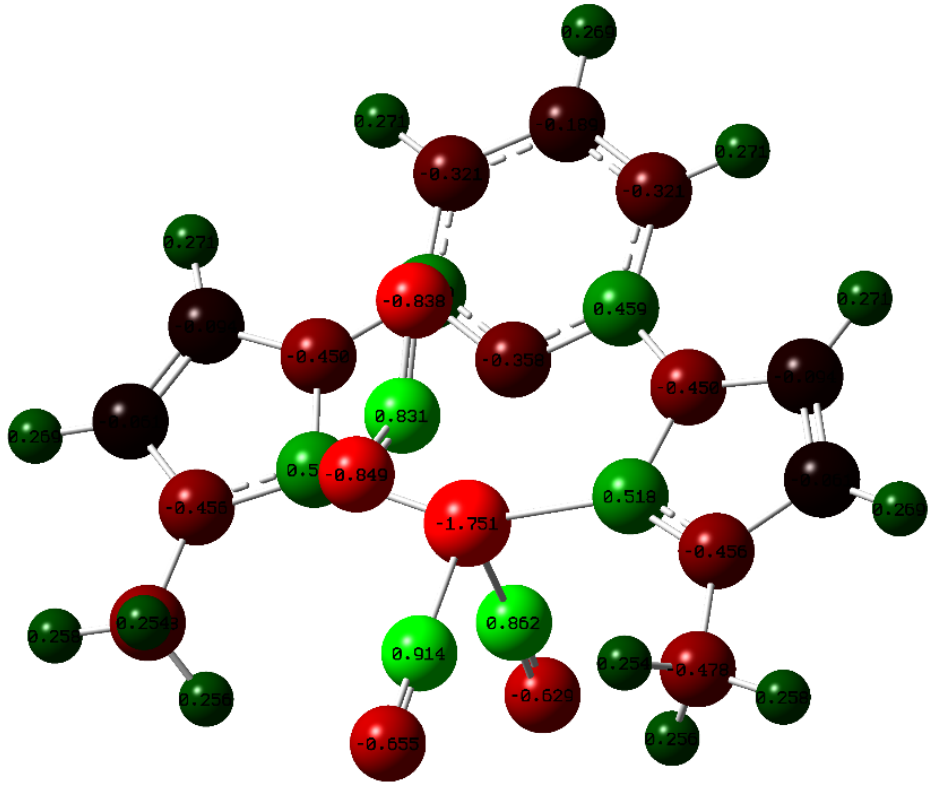

Figure S12. Charge density of **VI**.

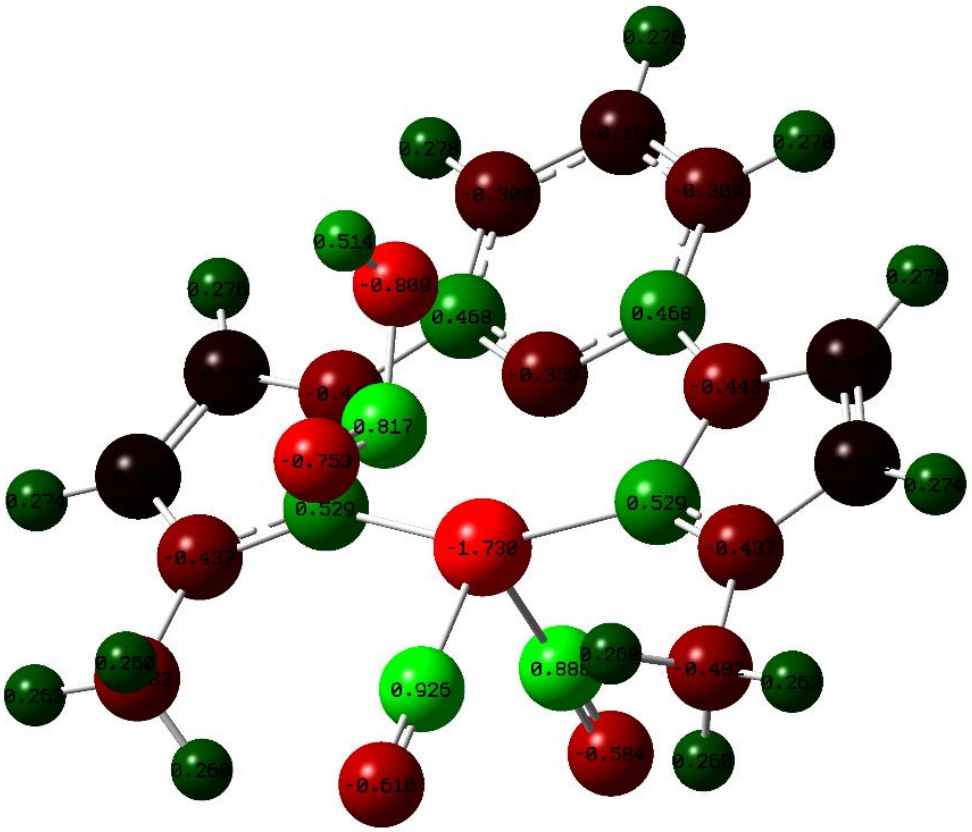

Figure S13. Charge density of **VII**.

Mechanism A Spin Densities

Spin Densities of Open-Shell Intermediates in Mechanism A

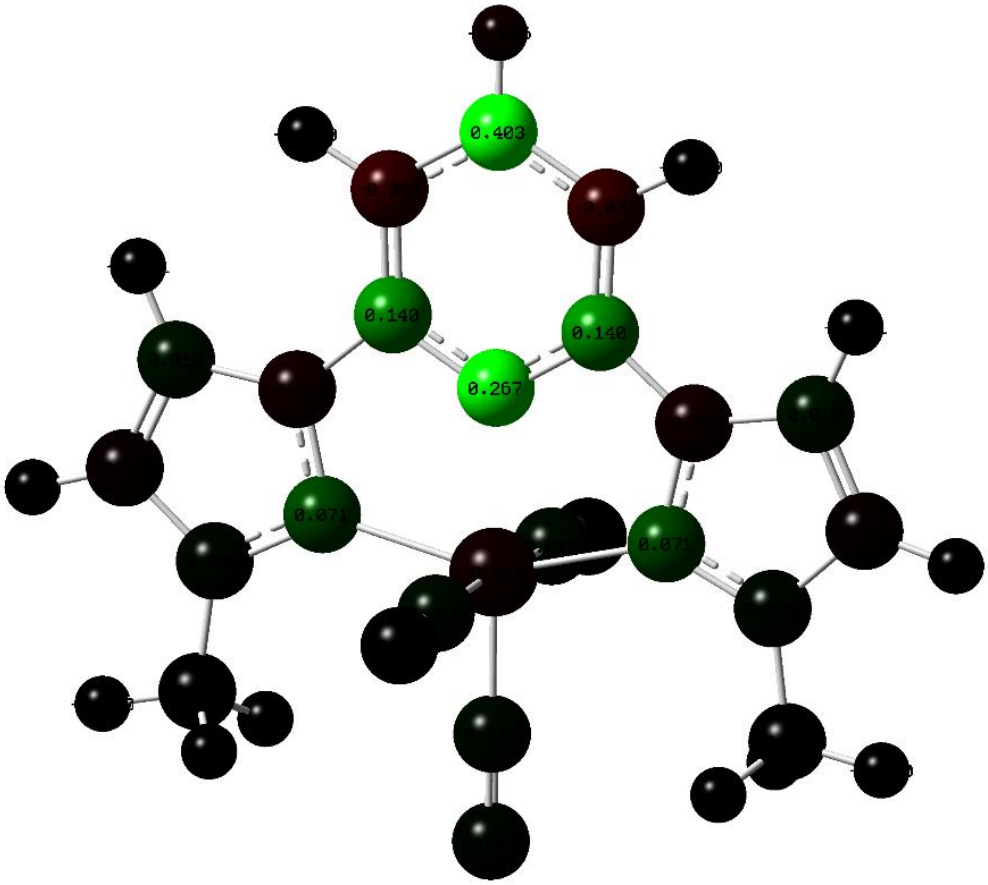

Figure S14. Spin density of **II**.

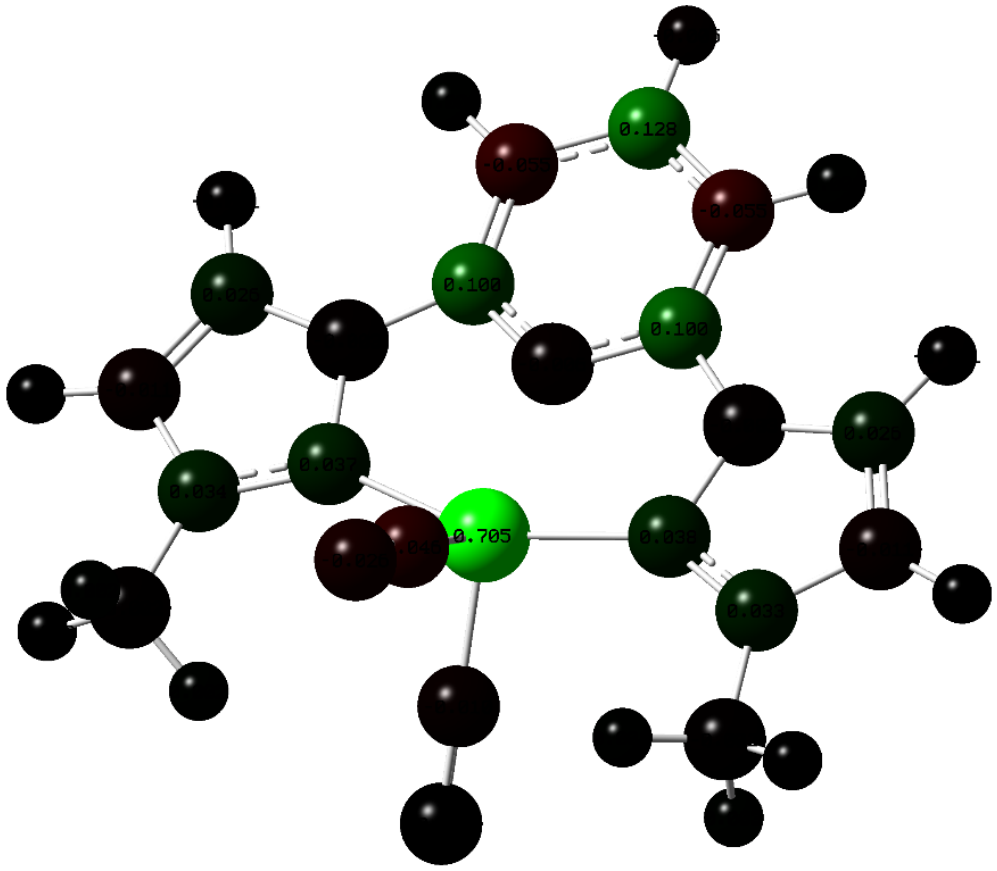

Figure S15. Spin density of **III**.

Mechanism B Charge Densities

Charge densities of intermediates participating in the proposed Mechanism B, as projected by NBO Natural Bonding Orbitals.

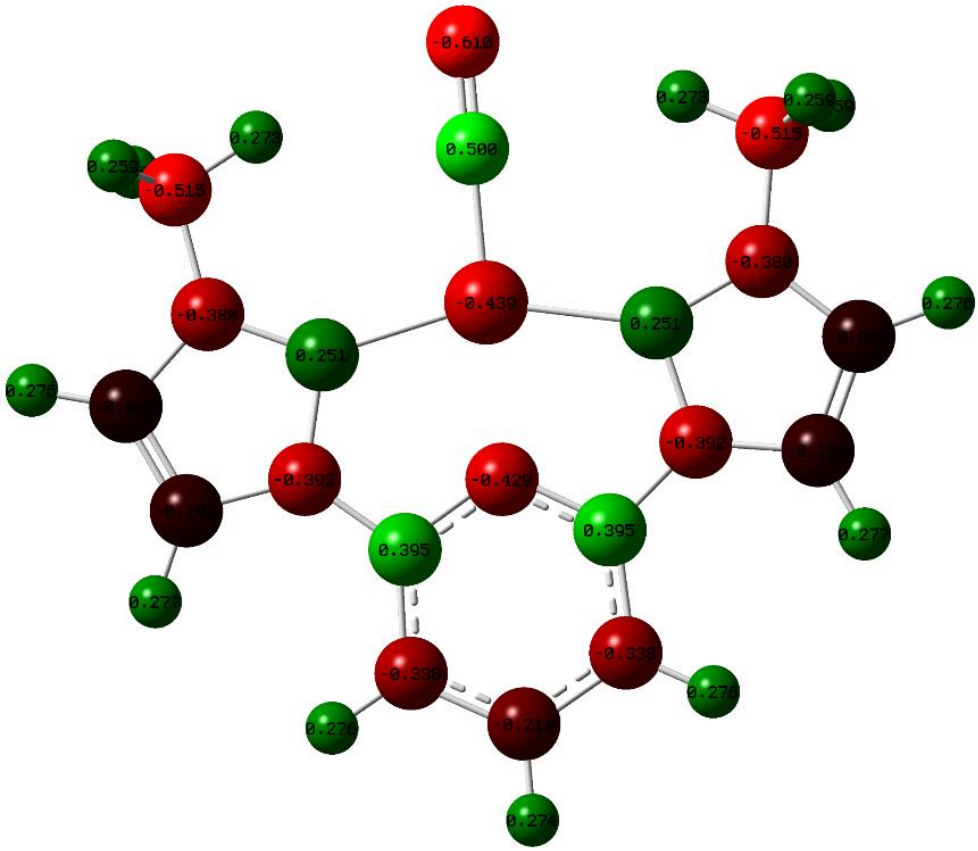

Figure S16. Charge density of **IV**.

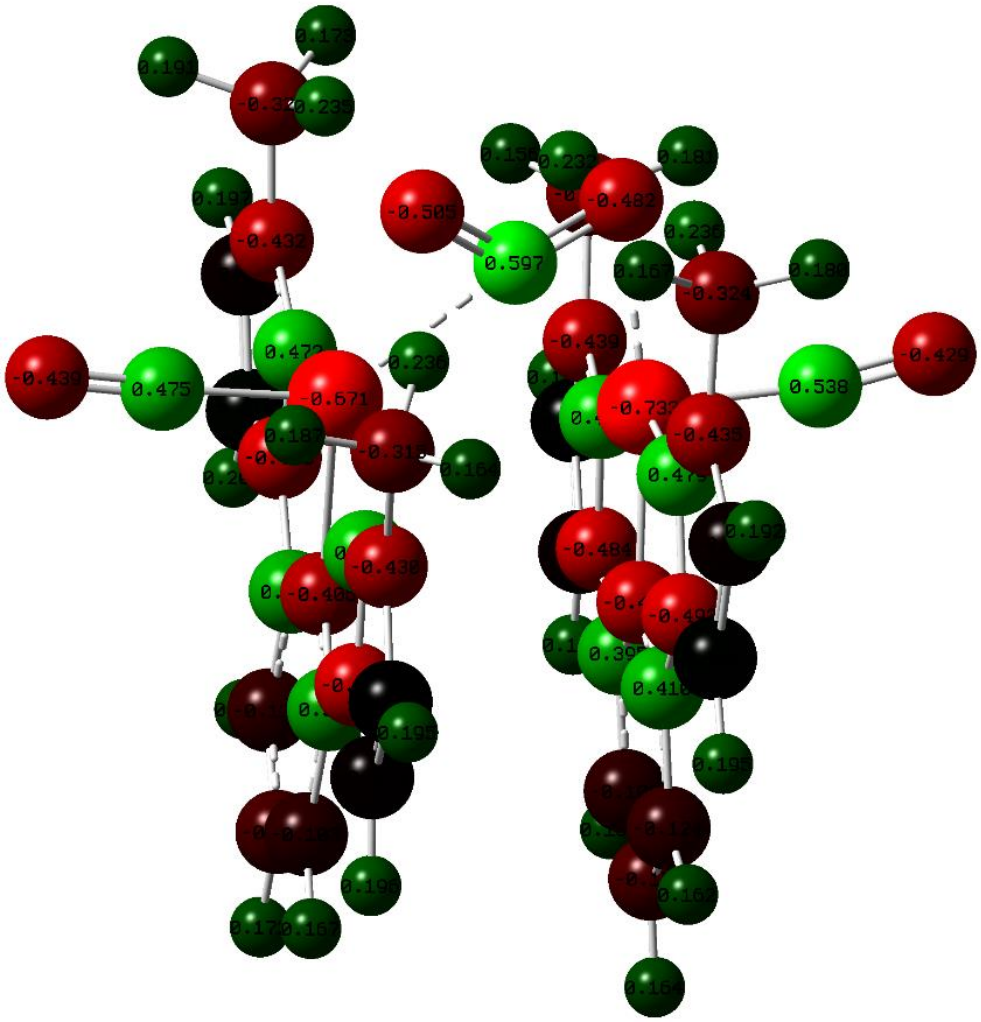

Figure S17. Charge density of **VIIIa**.

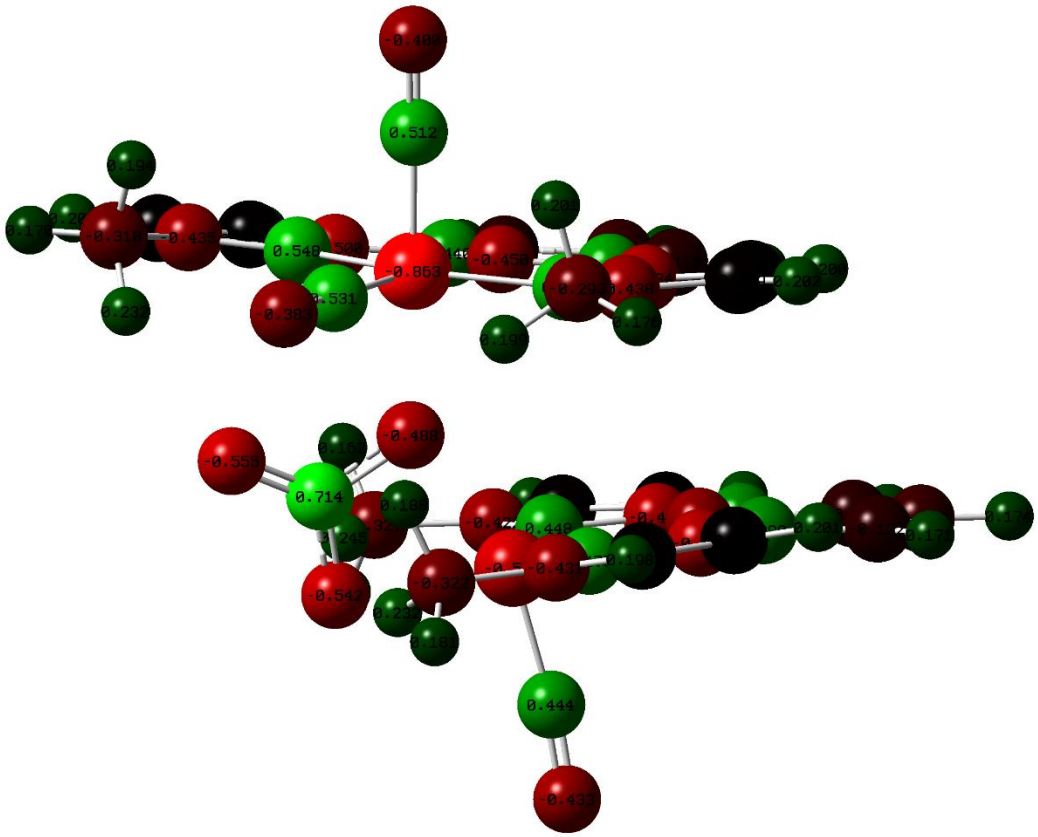

Figure S18. Charge density of **IXa**.

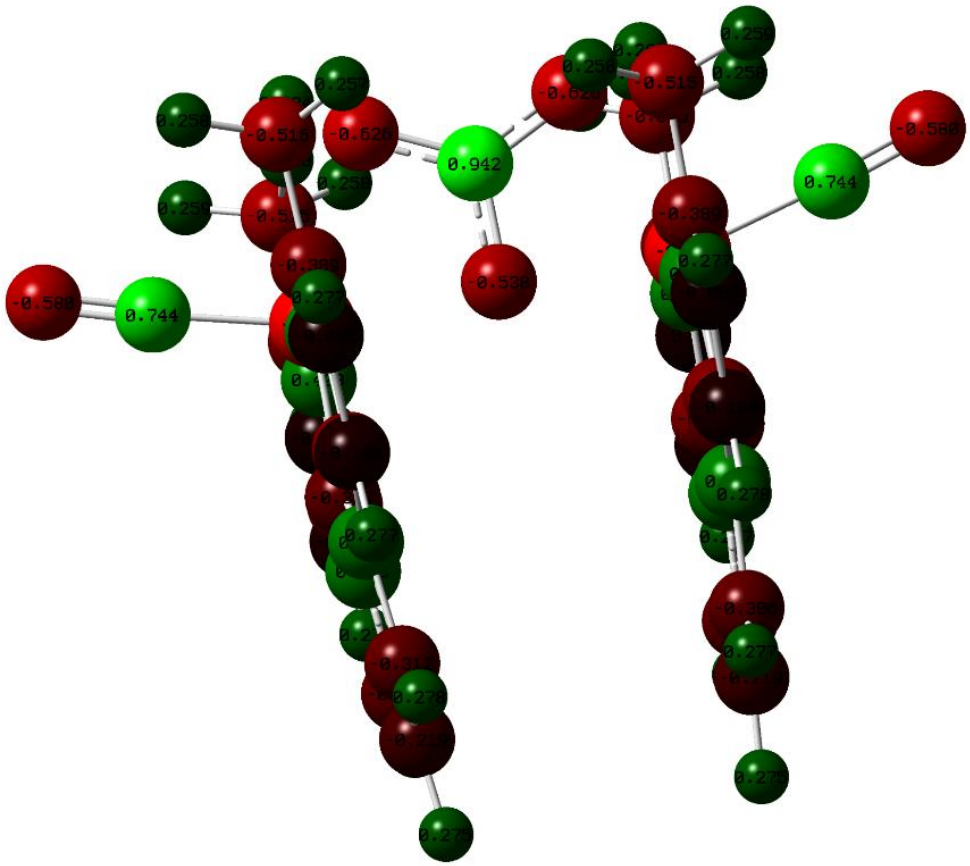

Figure S19. Charge density of **Xa**.

Mechanism C Charge Densities

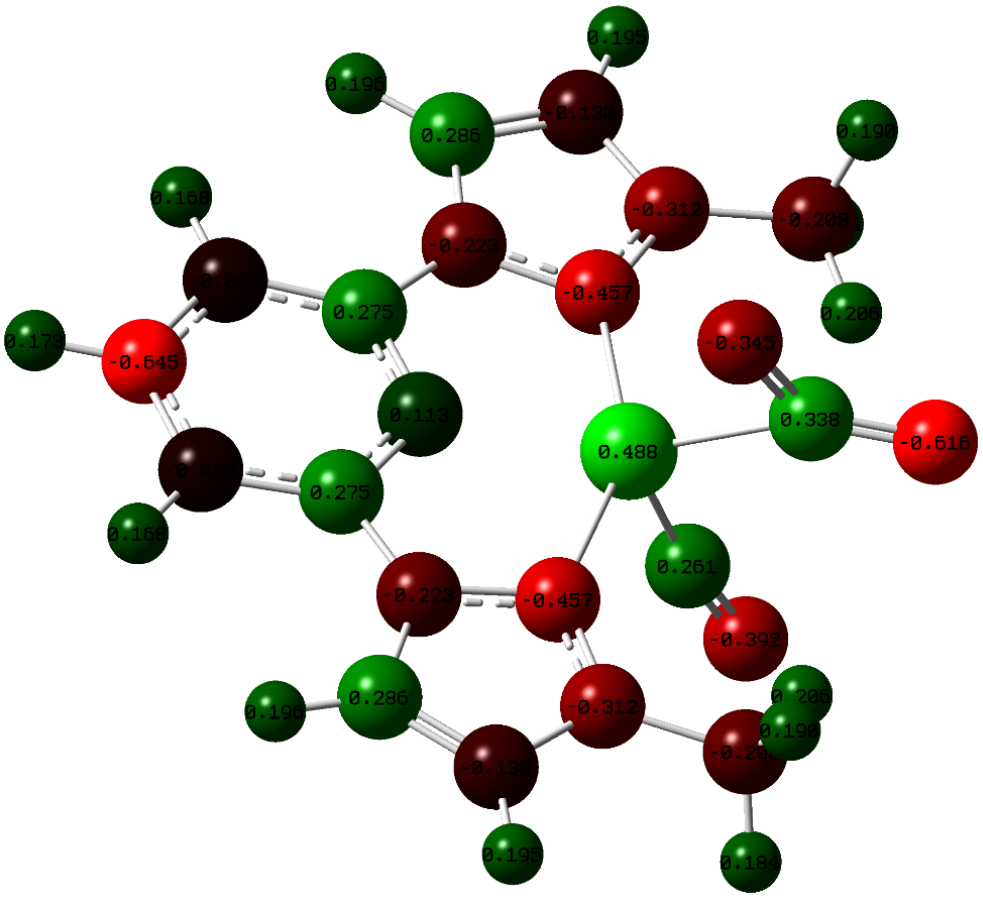

Figure S20. Charge density of **XI**.

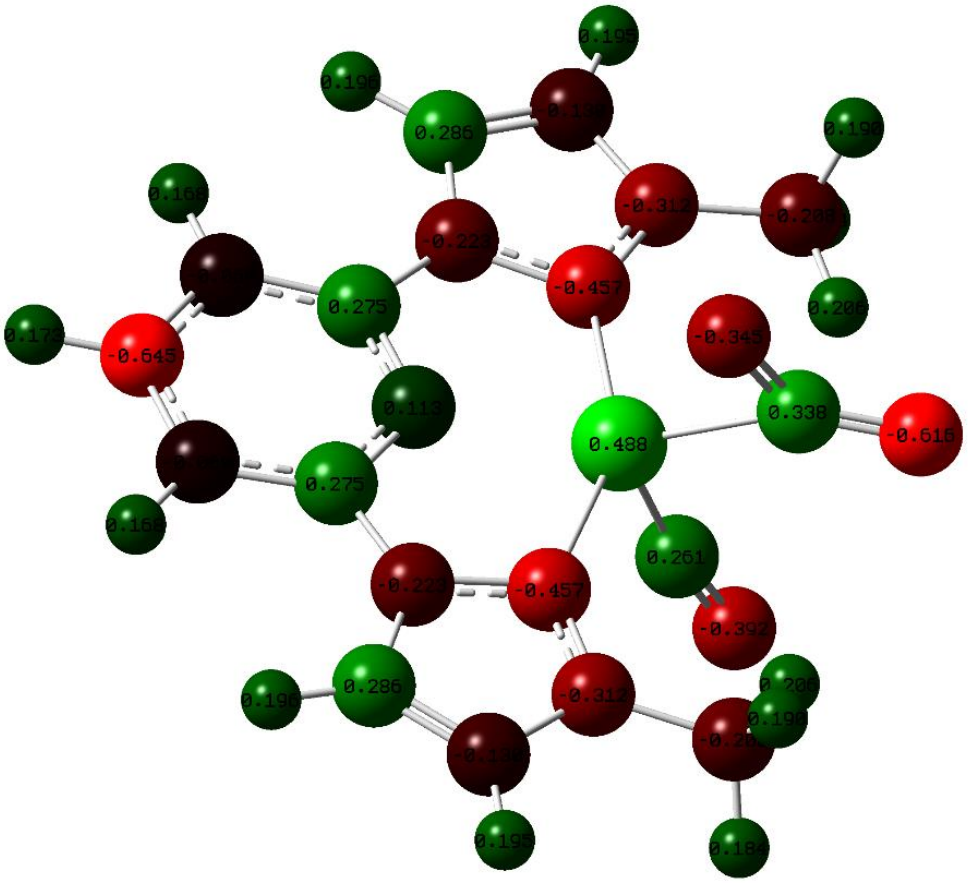

Figure S21. Charge density of **XII**.

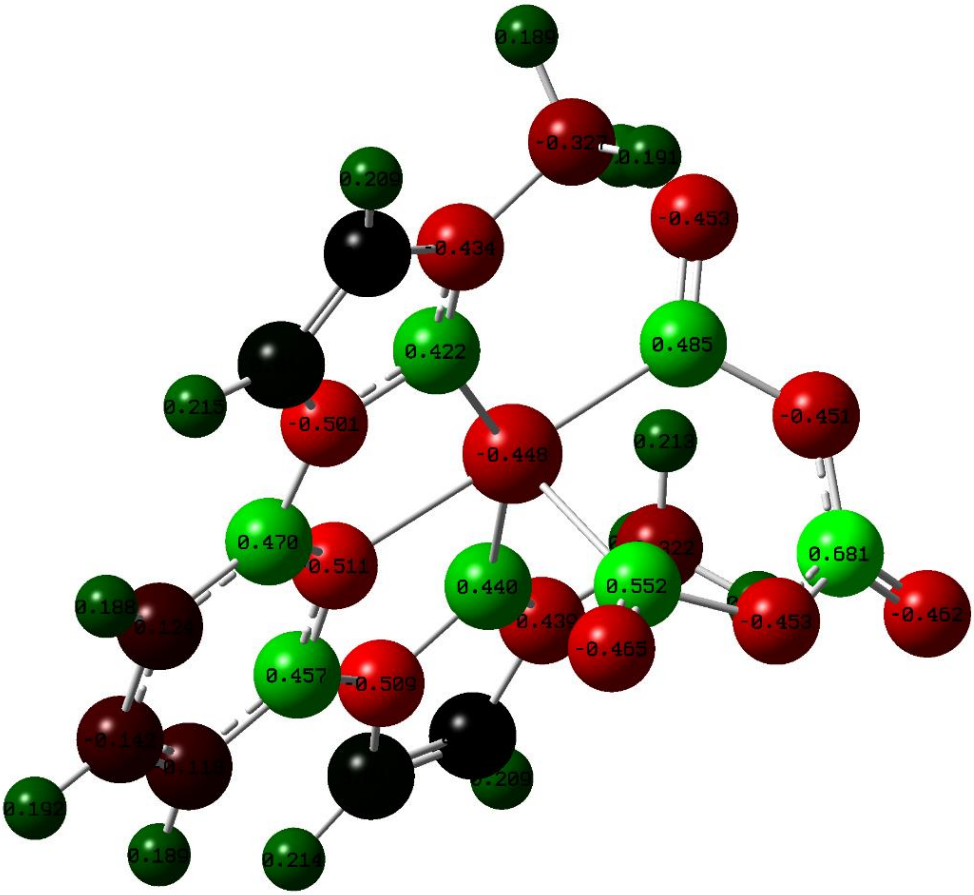

Figure S22. Charge density of **XIII**.

Salt Stabilization Geometry

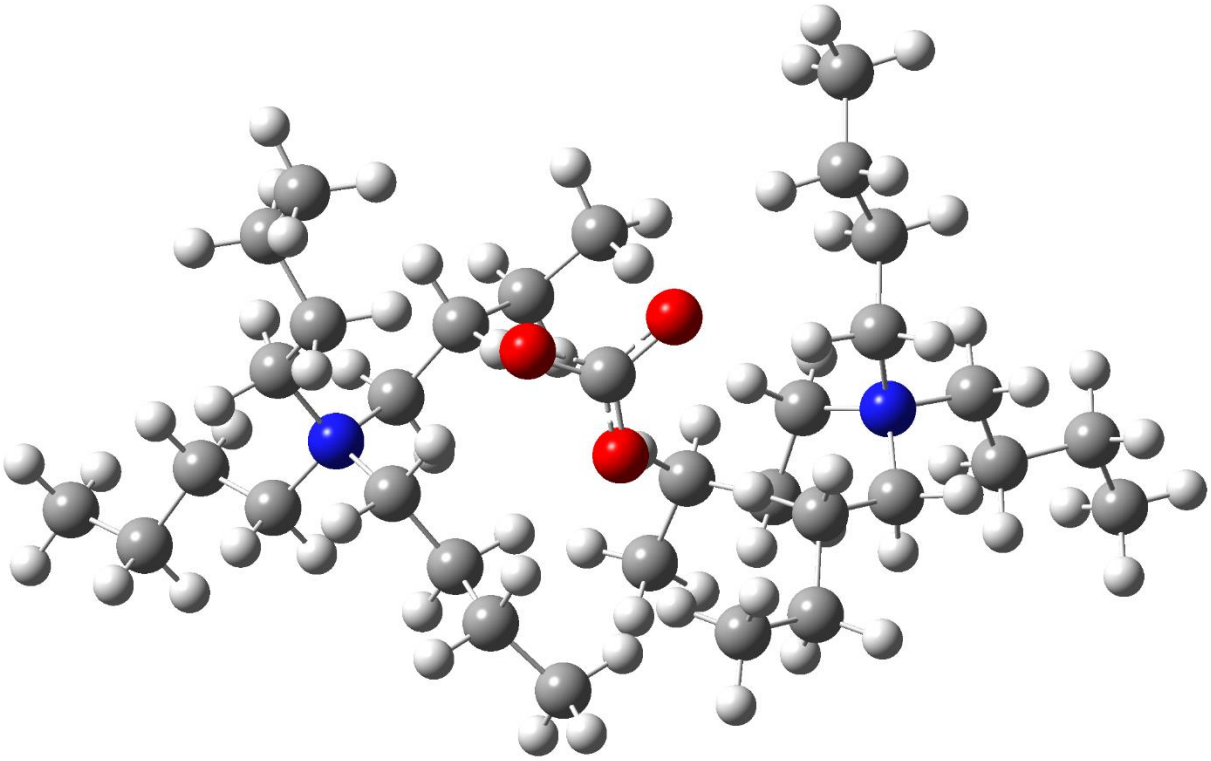

Figure S23. Geometry of $(N(n\text{-}Bu)_4)_2CO_3$.

Anti-ferromagnetism of IV

Anti-ferromagnetic behavior is common throughout various Mn-based complexes. As such, it is imperative to start a DFT calculation for such molecules with an appropriate guess wavefunction to converge at the global minimum energy for the respective molecule. In most of our computed geometries, no anti-ferromagnetism was observed. However, the square planar IV was found to have some extent of anti-ferromagnetic character, where the total spin multiplicity is a doublet, but the Mn atom is approximately quartet (spin-up) and the CNC ligand is approximately triplet (spin-down), as shown in Figure S24.

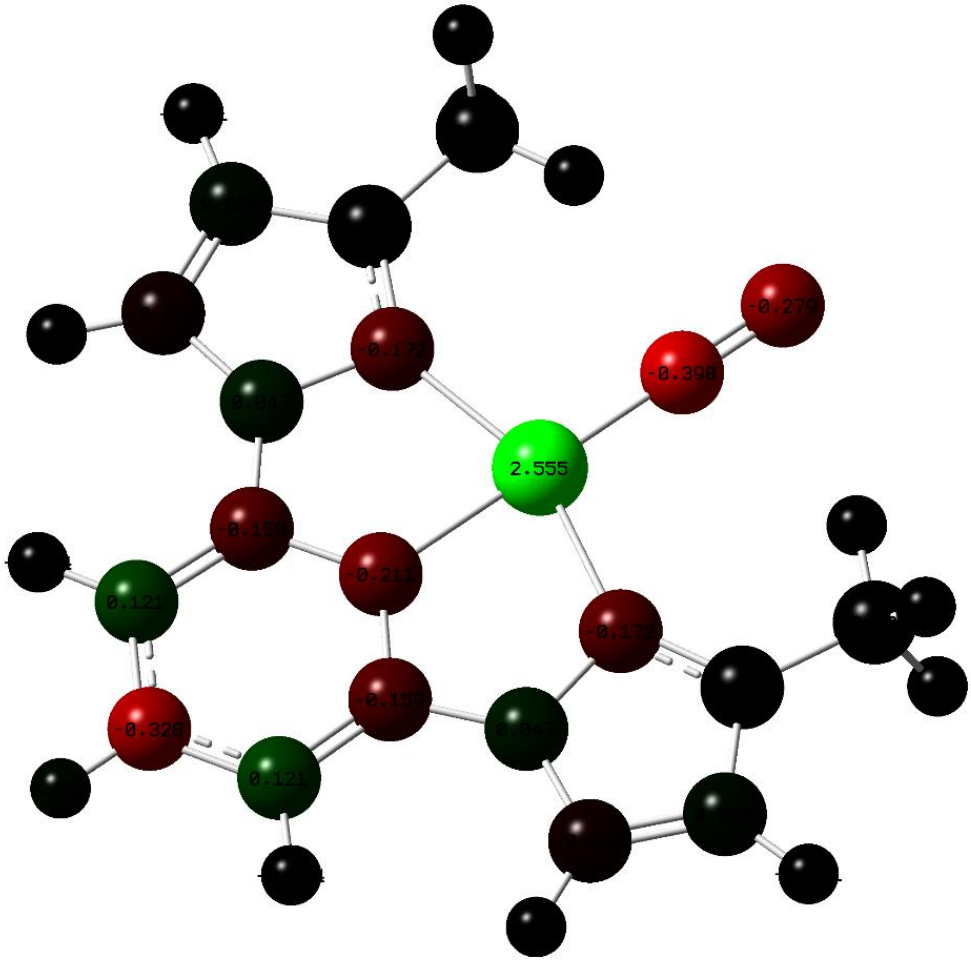

Figure S24. Spin population density plot for **IV**. This shows that the spin on Mn center is ~2.6 (almost a quartet), whereas the sum of spin densities on the CNC and CO ligands sums up to ~-1.6 (almost a triplet). The numbers are not meant to be meaningful quantitatively and should only be used for qualitative purposes.

Alternative pathway (b) for Mechanism B

The most likely pathway for Mechanism B is shown in Figure 2 of the main text. Here we show an alternative pathway for Mechanism B. This pathway shown in Figure S25 involves the coordination of 2 **IV**'s in an anti- manner, where the two complexes are facing each other rather than stacked on top of one another. The energetics indicate that pathway (a) shown in the main text is more favorable, possibly due to favorable π interactions from the overlapping space when the complexes are stacked on top of each other.

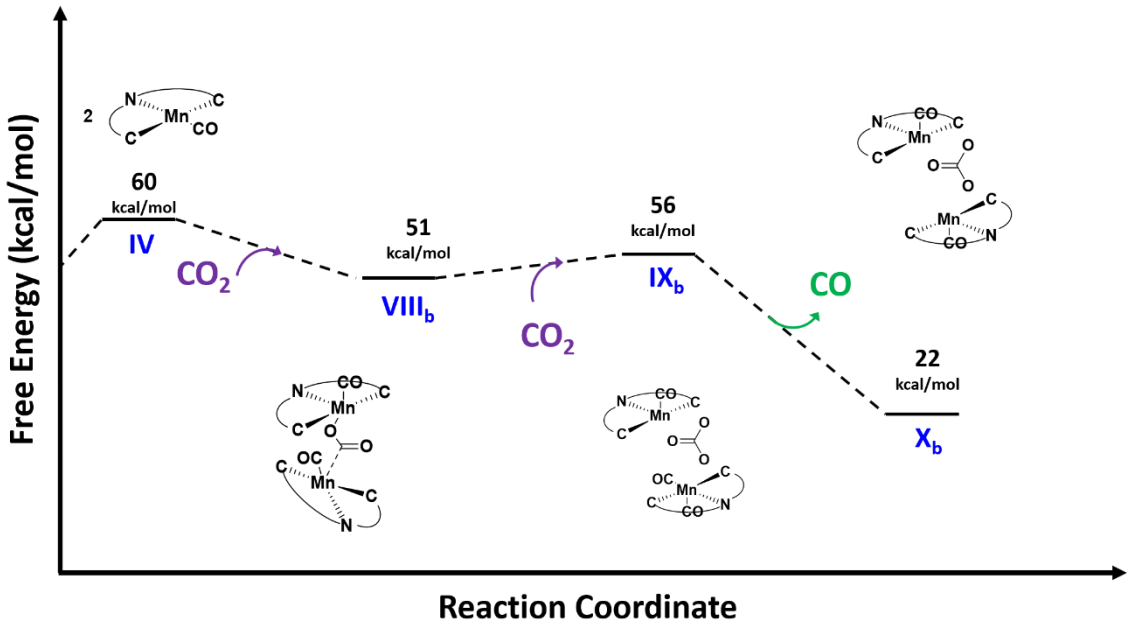

Figure S25. Alternative Pathway (b) for Mechanism B.

Benchmarking DFT methods

Appropriate benchmarking of DFT methods is necessary when dealing with systems of such complexity. As such we compared computed reaction energetics, reduction potentials, and pKa values via 3 different methods: MN15,[4-5] M06,[14] and wB97XD. Split basis-sets are used in these calculations where all Mn atoms are described using SDD pseudopotentials and all other atoms by 6-31+G(d,p). For Mechanism B, only MN15 calculations incorporate the appropriately sized 6-31+G(d,p), whereas M06 and wB97xd methodologies incorporate a smaller 6-31G(d) basis set as these take significantly shorter computational time to converge. An essential characteristic of these molecules is the Van der Waals interactions, which are inherently included in these functionals and are not added as corrections. We find that all these methods reproduce the same energies within 8 kcal/mol error (mean absolute error) and 0.16 V for reduction potentials. The mean absolute error drops to **<6** kcal/mol if the wB97XD results are ignored (they are incomplete due to difficulties converging the correct IV calculation). While the differences in ΔG_{rxn} of Mechanism C are largest, they all arrive at the same conclusion that this mechanism is highly unlikely due to the uphill nature of this pathway as predicted by all functionals. The error is notably large for the "sandwiching" step in Mechanism B. Nonetheless, the ΔG_{rxn} remains below zero indicating that this step is favorable regardless of the method used. In the main text, all reported energies are computed with the MN15 functional because it is parametrized to problems of multi-reference character. As such, we believe its energies and geometries are the most accurate of these three methods, in addition to the use of a larger basis set for Mechanism B. Table S2 summarizes these results.

Table S2. Summary of Reaction Free Energies and Reduction Potentials using various methods.

Reaction	**Free Energy / Reduction Potential**				**St. Dev.**
	M06	MN15	wB97XD		
$E^0(I/II)$	-2.23	-2.39	-2.42	vs Fc/Fc+	0.1
II --> III +CO	-3.88	-8.17	1.05	kcal/mol	4.6
II --> IV +2CO	13.71	3.14	-	kcal/mol	7.5
$E^0(III/V)$	-1.94	-2.14	-2.36	vs Fc/Fc+	0.2
$V + CO_2$ --> *VI*	7.89	4.39	-6.99	kcal/mol	7.8
VI --> VI$_{equatorial}$	12.87	13.06	11.07	kcal/mol	1.1
$VI + H^+$ --> *VII*	-50.32	-54.34	-58.92	kcal/mol	4.3
$VII + H^+$ -->*I* + H_2O	-47.15	-47.90	-37.57	kcal/mol	5.8
$2IV + CO_2$--> *VIIIa*	-2.74	-13.8	-	kcal/mol	7.8
VIIIa + CO_2 --> *IXa*	-19.54	-18.3	-3.63	kcal/mol	8.8
IXa ---> *Xa* + *CO*	14.57	0.3	-12.72	kcal/mol	13.6
IV + CO_2 -->*XI*	3	0.2	-	kcal/mol	2.0
IV + CO_2 -->*XII*	33.45	28.3	-	kcal/mol	3.6
XI + CO_2 -->*XIII*	47.43	13.8	27.87	kcal/mol	16.9
XII + CO_2 -->*XIII*	16.98	-14.4	3.51	kcal/mol	15.7
			Mean Absolute Error	ΔG_{rxn}	**9.0**
				E^0	**0.16**

Transition State Calculations

No Transition states were found for the following reactions of interest:

1) **V** + CO_2 → **VI**
2) **IV** + CO_2 → **XII**
3) **XII** + **IV** → **VIIIa**
4) **VIII$_a$** + CO_2 → **IXa**

To confirm our results we performed scan calculations along the reaction coordinates for each reaction of the 4 listed reactions. Due to the difficulty of converging scan calculations using split basis-sets, we employ the lanl2dz basis set for these scan calculations with the MN15 functional (T. H. Dunning Jr. and P. J. Hay, in Modern Theoretical Chemistry, Ed. H. F. Schaefer III, Vol. 3 (Plenum, New York, 1977) 1-28 and DOI: 10.1063/1.448799,

DOI: 10.1063/1.448975, DOI: 10.1063/1.448800)

The scans in addition to the geometries are discussed below.

1) **V** + CO_2 → **VI**

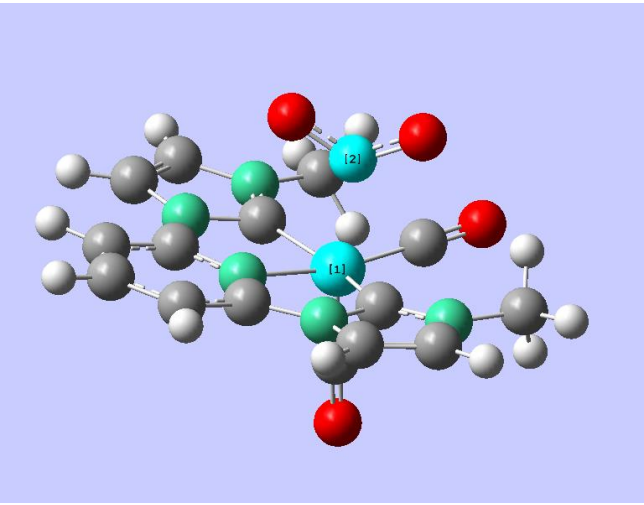

Figure S26. Structure of CO_2 approaching molecule **V** to form **VI**.

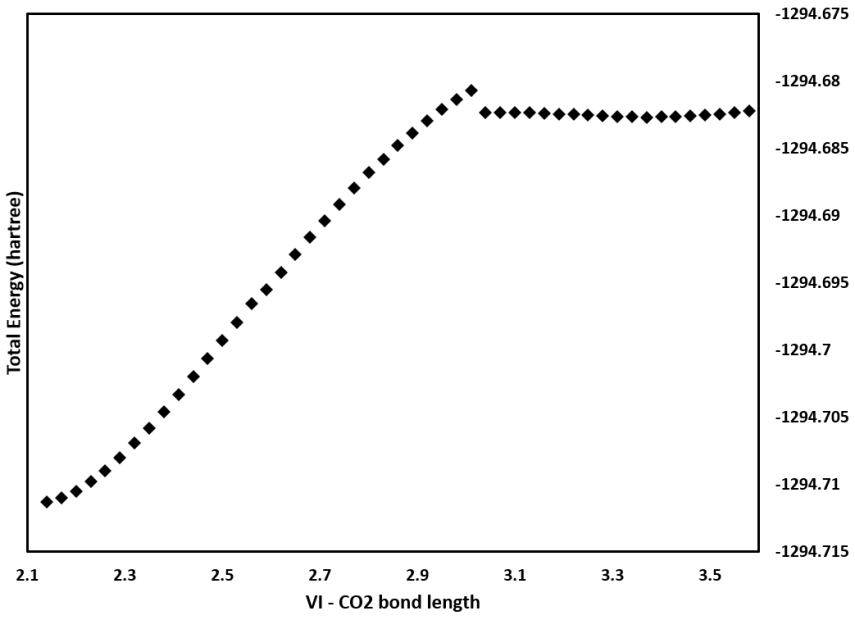

Figure S27. Total energy as a function of the scan coordinate – the distance between Mn and C atoms labelled 1 and 2, respectively, in Fig S26.

2) **IV** + CO_2 → **XII**

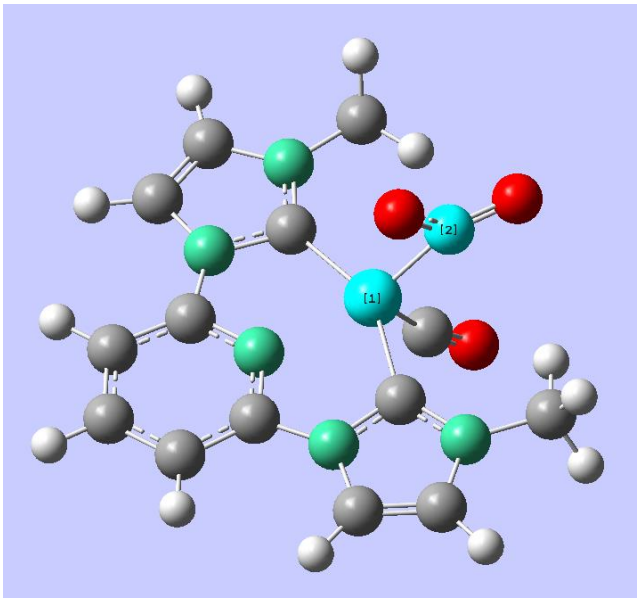

Figure S28. Structure of **CO_2** approaching molecule **IV** to form **XII**.

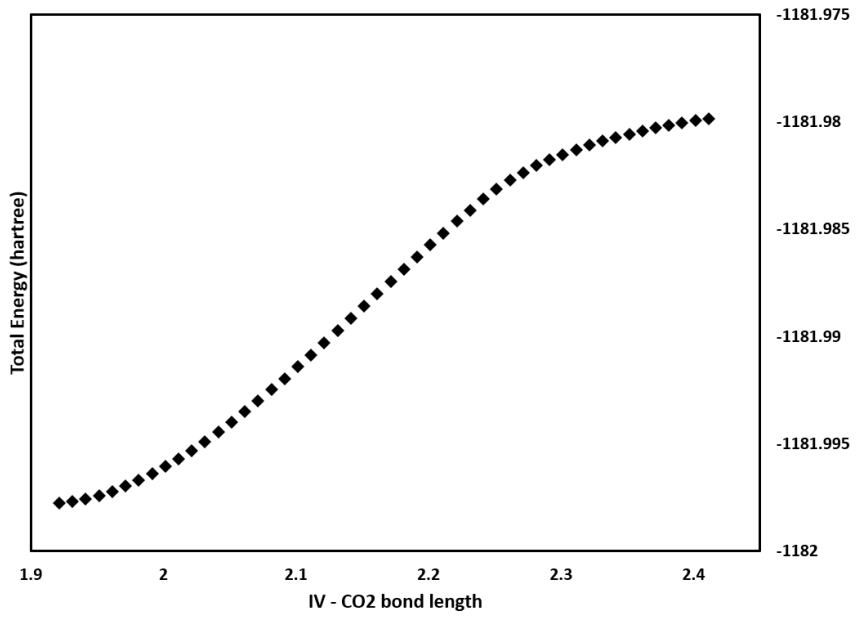

Figure S29. Scan along the Mn-C bond distance labelled **1** and **2**, respectively. Due to the monotonic behavior as the bond distance decreases, we can deduce that CO_2 insertion to **IV** is barrier-less.

3) **XII** + **IV** → **VIII**$_a$

For this reaction the scans are slightly more complicated. Here we perform a 3-dimensional scan of Mn-C (1-2) and Mn-O (3-4) bond distances. We find that there is a very small saddle point with a coarse scan, as shown in Fig S31. However, with a more refined scan around the predicted saddle point, the saddle point is essentially nonexistent.

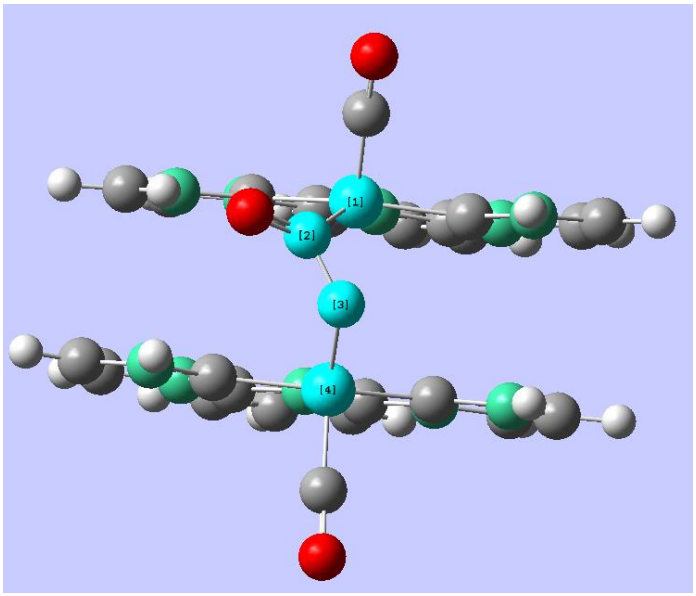

Figure S30. Molecule IV approaching XII.

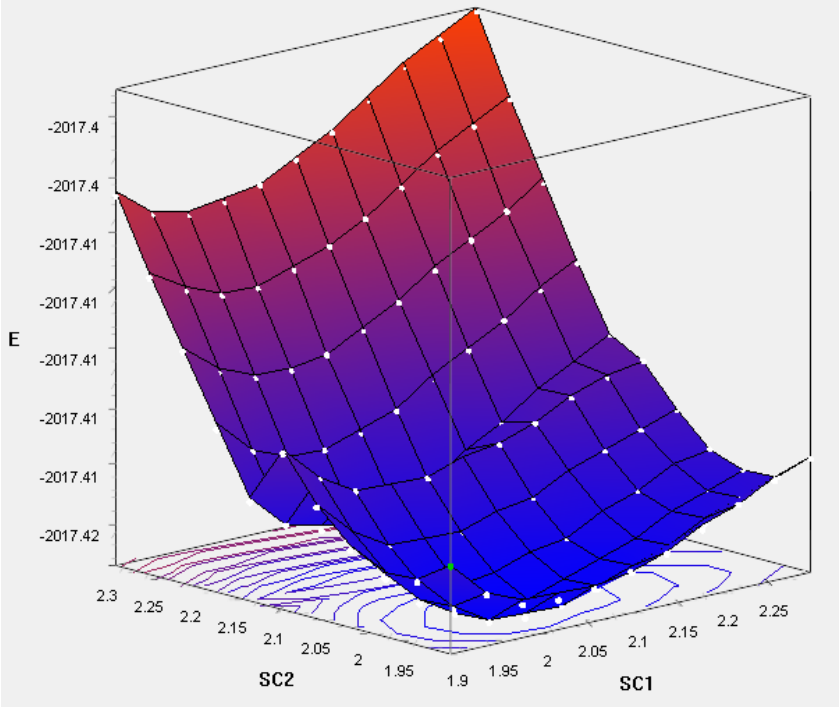

Figure S31. Three-dimensional scan of Mn-C and Mn-O bond distances. A tiny saddle point is observed around 2.05 Angstroms of scan coordinate 1 (Mn-C) and 2.15 Angstroms of scan coordinate 2 (Mn-O).

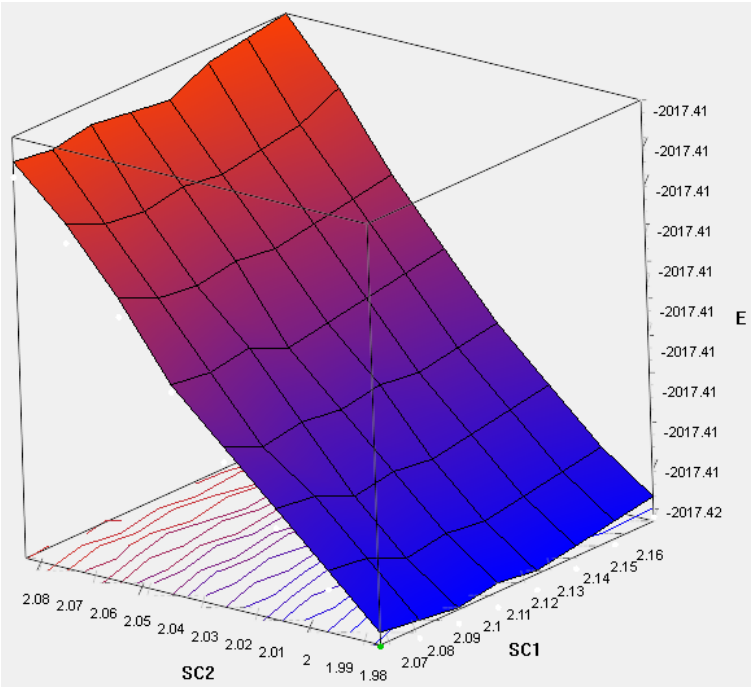

Figure S32. A more refined scan with more data points around the saddle point in Fig S31 showing that it is nonexistent. This indicates that this reaction monotonic along both scan coordinates and that this reaction is most likely barrier-less.

4) $\mathbf{VIII}_a + CO_2 \rightarrow \mathbf{IX}_a$

We split this reaction into 2 steps so that we can more closely analyze the transition state(s). The first step involves CO_2 approachin a Mn atom, and the second step involved the transfer of O atom from the just-reacted CO_2 on Mn to the previously sandwiched CO_2 to form a sandwiched carbonate and a CO on the Mn complex. As shown below, the first step is barrier-less as indicated by the monotonic behavior of the energy as we scan along the Mn-C bond distance.

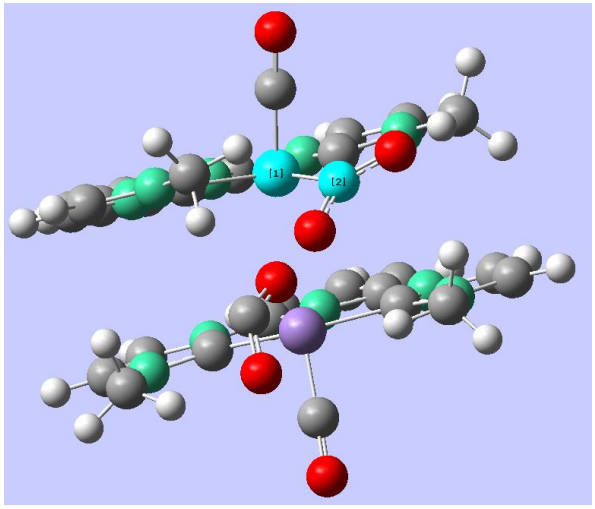

Figure S33. Part 1 of this reaction. CO_2 is approaching the top Mn atom in $VIII_a$.

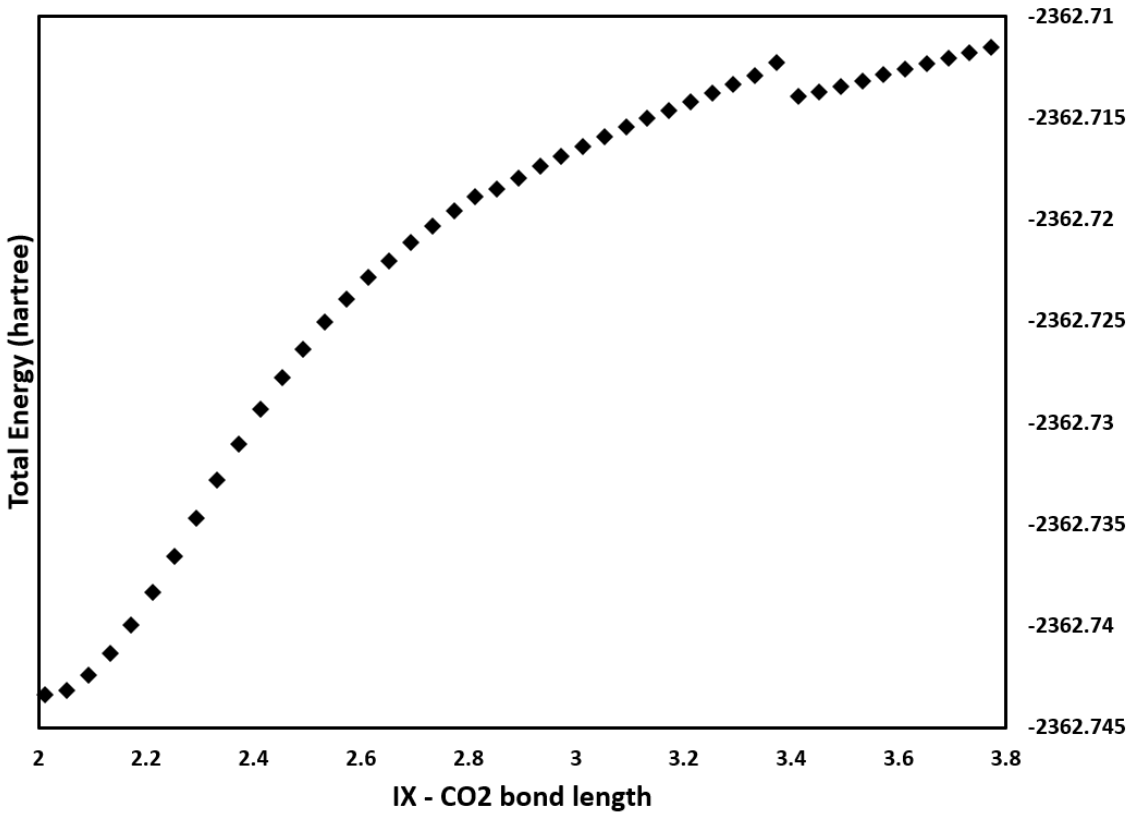

Figure S34. A monotonic reaction coordinate proves that this part of the reaction is barrier-less.

Molecular Coordinates

Molecular coordinates of intermediates in both reaction mechanisms are presented in this section. The coordinates are expressed in the xyz-Cartesian coordinate system. Zero-point energies (ZPEs) are reported for each molecule in units of Hartree/particle. ZPEs were calculated using MN15/6-31+G(d,p)/SDD(Mn) methodology, as appropriately discussed in Computational Details.

CO_3^{2-}
ZPE = -263.79

C	0	0.0008	0
O	-1.0263	0.7988	0
O	-0.1785	-1.2871	0
O	1.2048	0.4877	0

CO
ZPE = -113.20

C	0	0	-0.6512
O	0	0	0.4884

CO_2
ZPE = -188.39

C	0	0	0
O	0	0	1.1682
O	0	0	-1.1682

H_2O
ZPE = -76.34

O	0	0	0.1167
H	0	0.7711	-0.4669

H	0	-0.7711	-0.4669

I

ZPE = -1219.66

Mn	0	-0.7131	0
O	-0.0001	-0.8794	-2.9972
O	0	-3.6637	0.0001
N	0	1.3054	0
N	3.1442	-0.8781	0
N	2.2385	1.069	0
N	-2.2385	1.069	0
N	-3.1442	-0.8781	0
C	1.9418	-0.2778	0
C	-1.9418	-0.2778	0
C	-0.0001	-0.7871	-1.8481
C	0	-0.7871	1.8481
C	0	-2.5004	0.0001
C	3.3285	-2.328	0
H	2.8708	-2.76	-0.8929
C	3.6139	1.2901	0
C	1.1621	1.9662	0
C	1.2207	3.3553	0
H	2.1673	3.883	0
C	0	4.0373	0
H	0	5.1228	0
C	-1.2207	3.3553	0
H	-2.1674	3.883	0
C	-1.1621	1.9662	0
C	-3.6139	1.2901	-0.0001
H	-4.0557	2.2748	-0.0001
C	-4.1786	0.0598	-0.0001
H	-5.217	-0.2365	-0.0001
C	-3.3285	-2.3281	0
H	-2.8707	-2.76	-0.8929
H	-4.3966	-2.546	-0.0001
H	-2.8709	-2.76	0.8929
O	0.0001	-0.8796	2.9972
H	4.3966	-2.546	0
H	2.8708	-2.76	0.8929

C	4.1786	0.0599	0
H	4.0557	2.2749	0
H	5.217	-0.2365	0

II

ZPE = -1219.75

Mn	0	-0.7392	0
O	0.0008	-0.7708	3.0009
O	0.001	-3.6851	0.0001
N	-0.0003	1.2705	-0.0004
N	-3.1491	-0.8945	0
N	-2.2498	1.063	-0.0001
N	2.2494	1.0635	-0.0001
N	3.1492	-0.8938	0
C	-1.9432	-0.2757	0
C	1.9431	-0.2752	-0.0001
C	0	-0.7521	1.8443
C	-0.0002	-0.7532	-1.8443
C	0.0001	-2.514	0.0005
C	-3.3142	-2.3427	0.0001
H	-2.8495	-2.7733	0.891
C	-3.6245	1.2676	-0.0001
C	-1.1754	1.9781	-0.0001
C	-1.2299	3.3483	0
H	-2.1865	3.864	0.0002
C	-0.0006	4.0744	0.0001
H	-0.0007	5.1584	0.0002
C	1.2289	3.3486	0
H	2.1854	3.8645	0.0001
C	1.1747	1.9784	-0.0002
C	3.624	1.2684	-0.0001
H	4.0719	2.2508	-0.0002
C	4.1863	0.0327	0
H	5.2237	-0.2685	0
C	3.3146	-2.3419	0.0001
H	2.85	-2.7726	0.8911
H	4.3802	-2.5756	0
H	2.8496	-2.7728	-0.8905
O	0.0011	-0.7726	-3.0009
H	-4.3798	-2.5766	-0.0001

H	-2.8492	-2.7735	-0.8905
C	-4.1865	0.0317	0
H	-4.0726	2.2498	-0.0002
H	-5.2238	-0.2698	0

III

ZPE = -1106.55

Mn	-0.0003	-0.7168	-0.0708
O	-0.0001	-3.3375	-1.405
N	0.0008	1.2843	-0.0462
N	3.1325	-0.8901	-0.1213
N	2.236	1.0658	-0.0762
N	-2.2346	1.0678	-0.0785
N	-3.1322	-0.8877	-0.1238
C	1.9155	-0.2869	-0.1212
C	-1.9149	-0.285	-0.1239
C	-0.004	-1.5328	1.4813
C	-0.0004	-2.2744	-0.8866
C	3.3013	-2.3353	-0.1788
H	3.0956	-2.7062	-1.1873
C	3.614	1.275	-0.0544
C	1.1662	1.9602	-0.0443
C	1.2223	3.3488	-0.0206
H	2.1702	3.8758	-0.018
C	0.0019	4.0363	-0.0056
H	0.0024	5.1218	0.0126
C	-1.219	3.3499	-0.0217
H	-2.1665	3.8777	-0.0201
C	-1.1642	1.9612	-0.0454
C	-3.6126	1.2776	-0.0554
H	-4.0635	2.2578	-0.0167
C	-4.1689	0.0424	-0.0858
H	-5.207	-0.257	-0.0817
C	-3.3005	-2.3331	-0.1785
H	-3.0767	-2.7077	-1.1817
H	-4.3303	-2.5844	0.0815
H	-2.6177	-2.801	0.5355
O	-0.0073	-2.125	2.5047
H	4.3259	-2.5884	0.0994
H	2.6052	-2.8049	0.521
C	4.1697	0.0395	-0.0849
H	4.0654	2.2549	-0.0157
H	5.2076	-0.2605	-0.0806

IV

ZPE = -993.32

Mn	0	0.8935	0
N	0	-1.0882	0
N	3.2522	0.991	0
N	2.2639	-0.9221	0
N	-2.2639	-0.9221	0
N	-3.2522	0.991	0
C	2.0085	0.4371	0
C	-2.0085	0.4371	0
C	3.5194	2.4229	0
H	4.0874	2.7007	-0.8918
C	3.6267	-1.1894	0
C	1.1686	-1.7988	0
C	1.2196	-3.1773	0
H	2.1709	-3.7006	0
C	0	-3.8865	0
H	0	-4.9711	0
C	-1.2196	-3.1773	0
H	-2.1709	-3.7006	0
C	-1.1686	-1.7988	0
C	-3.6267	-1.1894	0
H	-4.0354	-2.1885	0
C	-4.2423	0.021	0
H	-5.2931	0.2725	0
C	-3.5194	2.4229	0
H	-2.563	2.9462	-0.0002
H	-4.0874	2.7007	-0.8918
H	-4.0872	2.7007	0.8919
H	4.0872	2.7008	0.8919
H	2.563	2.9462	-0.0002
C	4.2423	0.021	0
H	4.0354	-2.1885	0
H	5.2931	0.2725	0
C	0	2.6443	-0.0001
O	0	3.8366	0.0003

V

ZPE = -1106.66

Mn	0	0.6998	0
O	0.0053	2.8255	2.0149
N	0	-1.2694	0
N	3.1133	0.8852	0.0002
N	2.2292	-1.0923	-0.0007
N	-2.2292	-1.0924	0.0008
N	-3.1133	0.8851	-0.0001
C	1.8832	0.2652	-0.0008
C	-1.8832	0.2652	0.0008
C	-0.0025	1.9184	-1.2345
C	0.0025	1.9184	1.2345
C	3.2529	2.3283	-0.0021
H	2.7716	2.7553	0.8842
C	3.6143	-1.2791	-0.0002
C	1.1689	-1.9804	-0.0004
C	1.2168	-3.3673	-0.0004
H	2.1702	-3.888	-0.0008
C	0.0001	-4.0698	0
H	0.0001	-5.1557	0
C	-1.2167	-3.3674	0.0004
H	-2.1701	-3.8881	0.0007
C	-1.1689	-1.9804	0.0004
C	-3.6143	-1.2792	0.0002
H	-4.0808	-2.2532	-0.0001
C	-4.1538	-0.0346	0.0003
H	-5.1904	0.2729	-0.0002
C	-3.253	2.3283	0.0022
H	-2.7733	2.7522	0.891
H	-4.3136	2.5892	0.0017
H	-2.7716	2.7553	-0.8841
O	-0.0055	2.8251	-2.0153
H	4.3136	2.5893	-0.0016
H	2.7733	2.7523	-0.8909
C	4.1538	-0.0345	-0.0003

VI

ZPE = -1295.06

Mn	-0.0004	-0.6949	-0.2579
O	-0.0032	-3.5806	0.26
N	0.0005	1.3065	-0.3321

N	-3.1149	-0.8754	-0.017
N	-2.2235	1.0768	-0.1548
N	2.2243	1.0748	-0.1556
N	3.114	-0.8783	-0.0179
C	-1.9004	-0.275	-0.1218
C	1.9001	-0.2767	-0.1226
C	-0.0007	-1.0573	-1.9961
C	-0.001	-2.4162	0.0686
C	-3.2847	-2.3193	0.0603
H	-4.3501	-2.5546	0.0313
C	-3.5987	1.2902	-0.0583
C	-1.1557	1.9697	-0.216
C	-1.2166	3.3587	-0.1227
H	-2.1648	3.88	-0.0476
C	0.0018	4.045	-0.0968
H	0.0023	5.1286	-0.0239
C	1.2196	3.3576	-0.1231
H	2.1683	3.878	-0.0483
C	1.1573	1.9687	-0.2163
C	3.5997	1.287	-0.059
H	4.0511	2.2677	-0.0644
C	4.1519	0.0538	0.0267
H	5.1865	-0.246	0.1116
C	3.2824	-2.3222	0.06
H	2.8497	-2.7073	0.9882
H	4.3476	-2.5586	0.0311
H	2.7806	-2.7989	-0.7863
O	-0.0019	-1.3649	-3.1351
H	-2.7833	-2.7961	-0.7861
H	-2.8525	-2.7052	0.9885
C	-4.152	0.0575	0.0275
H	-4.0492	2.2713	-0.0637
H	-5.1869	-0.2413	0.1125
C	0.001	-0.425	1.8837
O	0.0053	0.7587	2.3427
O	-0.0024	-1.4576	2.6301

VII

ZPE = -1295.54

Mn	-0.0001	-0.7018	-0.2243
O	-0.0023	-3.6188	0.0928

N	0.0007	1.3111	-0.2404
N	-3.1277	-0.8741	-0.0653
N	-2.2304	1.0755	-0.1458
N	2.2316	1.0736	-0.1444
N	3.1274	-0.8767	-0.0643
C	-1.919	-0.2747	-0.1393
C	1.9192	-0.2763	-0.1381
C	0.0004	-0.9138	-2.0087
C	-0.0008	-2.4523	-0.041
C	-3.2999	-2.3217	-0.0174
H	-4.3663	-2.5516	-0.0077
C	-3.6057	1.2922	-0.0734
C	-1.1581	1.972	-0.175
C	-1.2183	3.3616	-0.11
H	-2.1655	3.8873	-0.0648
C	0.0019	4.0448	-0.0883
H	0.0023	5.1294	-0.0374
C	1.2214	3.3605	-0.1092
H	2.169	3.8854	-0.0634
C	1.1601	1.971	-0.1743
C	3.6071	1.2893	-0.0721
H	4.0542	2.2718	-0.0649
C	4.165	0.0568	-0.0225
H	5.2012	-0.2426	0.0366
C	3.2987	-2.3244	-0.0169
H	2.8326	-2.7273	0.8863
H	4.3649	-2.5551	-0.0094
H	2.8336	-2.7817	-0.8937
O	0.0008	-1.1097	-3.1624
H	-2.8371	-2.7794	-0.8953
H	-2.8322	-2.7248	0.8847
C	-4.1646	0.0602	-0.0236
H	-4.052	2.2751	-0.0664
H	-5.201	-0.2383	0.0356
C	-0.0019	-0.6256	1.8134
O	0.0022	0.6415	2.3727
O	-0.0066	-1.5505	2.6373
H	0.0005	0.5123	3.3424

VIII

ZPE = -2175.10

Mn	-0.4249	-1.0169	-1.5025
N	-0.814	1.1935	-1.3167
N	-3.5183	-1.5531	-0.8773
N	-2.9274	0.5119	-0.9414
N	1.3653	1.362	-1.8703
N	2.6507	-0.3268	-2.1892
C	-2.4257	-0.7782	-1.0616
C	1.3768	-0.0238	-1.8428
C	-0.7458	-1.0161	-3.2383
C	-3.4872	-3.0078	-0.942
H	-3.9687	-3.4338	-0.0566
C	-4.3009	0.5083	-0.7015
C	-2.0608	1.6051	-1.1369
C	-2.4068	2.9569	-1.1889
H	-3.4236	3.2999	-1.0277
C	-1.373	3.8543	-1.4854
H	-1.5946	4.9161	-1.541
C	-0.0646	3.4156	-1.7294
H	0.7287	4.1127	-1.979
C	0.1579	2.0435	-1.6275
C	2.6089	1.8843	-2.229
H	2.8082	2.9439	-2.2894
C	3.4136	0.8147	-2.4318
H	4.4569	0.7611	-2.7085
C	3.1123	-1.6967	-2.3695
H	2.4073	-2.3531	-1.8502
H	4.1152	-1.8089	-1.9469
H	3.1393	-1.955	-3.4328
O	-0.9358	-1.0922	-4.4053
H	-4.0028	-3.3633	-1.8387
H	-2.4396	-3.3189	-0.972
C	-4.6695	-0.7931	-0.6601
H	-4.8779	1.4111	-0.5672
H	-5.6356	-1.2473	-0.4923
Mn	0.4249	-1.0151	1.5031
N	0.8146	1.1948	1.3162
N	-2.6506	-0.3236	2.19
N	-1.3647	1.3644	1.8698
N	2.9278	0.5123	0.9412
N	3.5179	-1.5529	0.8786

C	-1.3767	-0.0214	1.8436
C	2.4257	-0.7775	1.0623
C	-3.1129	-1.6932	2.3714
H	-3.1407	-1.9503	3.435
C	-2.6081	1.8875	2.2278
C	-0.1571	2.0454	1.6262
C	0.0658	3.4175	1.7267
H	-0.7273	4.1151	1.9755
C	1.3743	3.8556	1.482
H	1.5961	4.9174	1.5365
C	2.4078	2.9577	1.1863
H	3.4246	3.3003	1.0245
C	2.0615	1.6059	1.1358
C	4.3013	0.508	0.7013
H	4.8786	1.4105	0.5666
C	4.6694	-0.7936	0.6609
H	5.6354	-1.2482	0.4936
C	3.4861	-3.0076	0.9445
H	4.0013	-3.3625	1.8417
H	3.9675	-3.4346	0.0596
H	2.4383	-3.3181	0.9746
H	-4.1155	-1.8055	1.9483
H	-2.4078	-2.3503	1.8532
C	-3.4133	0.8184	2.4314
H	-2.8071	2.9473	2.2873
H	-4.4566	0.7654	2.708
C	0.746	-1.0156	3.2387
O	0.9363	-1.0926	4.4056
O	0.2078	-3.1513	-1.1026
C	-0.0017	-2.5456	0
O	-0.2118	-3.1484	1.104

IXa

ZPE = -2363.53

Mn	1.9971	-0.8632	-0.5577
N	1.0499	0.6457	-1.4943

N	-0.1226	-3.0012	-1.5238
N	-0.4233	-0.9505	-2.0763
N	2.7324	1.8892	-0.6636
N	4.3906	0.9751	0.3467
C	0.3912	-1.7692	-1.3121
C	3.2032	0.6696	-0.2086
C	2.9583	-1.416	-1.9164
C	0.4716	-4.2208	-0.9888
H	-0.2318	-5.0457	-1.1172
C	-1.4028	-1.6726	-2.7535
C	-0.0888	0.4077	-2.1448
C	-0.7831	1.4139	-2.8124
H	-1.6989	1.2086	-3.3575
C	-0.2557	2.7057	-2.7228
H	-0.7683	3.5242	-3.2195
C	0.9094	2.9724	-1.9953
H	1.3076	3.9785	-1.9129
C	1.535	1.884	-1.3923
C	3.6188	2.9254	-0.3746
H	3.4423	3.9551	-0.6475
C	4.6595	2.3409	0.2668
H	5.5648	2.7697	0.6711
C	5.2584	-0.0213	0.9658
H	4.6985	-0.5138	1.7638
H	6.1411	0.4797	1.3671
H	5.5679	-0.7561	0.2173
O	3.6207	-1.8034	-2.8051
H	1.405	-4.4482	-1.5125
H	0.681	-4.0884	0.0747
C	-1.207	-2.9659	-2.4026
H	-2.141	-1.2137	-3.395
H	-1.7454	-3.8596	-2.6834
O	2.5665	-0.2829	2.5781
C	1.3881	0.0429	2.2884
O	0.8857	-0.1306	1.0661
O	0.541	0.5535	3.1255
Mn	-1.1112	0.3707	1.6099
C	-1.6913	-1.611	1.3184
C	-1.3297	2.285	0.6954
C	-2.4566	0.7187	2.684

N	-1.3139	-2.8131	1.8054
N	-2.6816	-1.9308	0.4068
N	-2.3685	2.4935	-0.199
N	-0.8051	3.5225	0.8464
O	-3.2794	0.9501	3.5058
C	-0.2379	-2.9644	2.7784
C	-2.0469	-3.8577	1.2419
C	-2.9155	-3.3043	0.3618
C	-3.3106	-0.8894	-0.3076
C	-3.1472	1.3953	-0.619
C	-2.4773	3.8337	-0.5629
C	-1.4866	4.4798	0.0978
C	0.3685	3.7887	1.6681
H	-0.5095	-3.7186	3.5205
H	0.6939	-3.2564	2.2815
H	-0.0876	-1.9972	3.2654
H	-1.8822	-4.8908	1.5135
H	-3.6487	-3.7577	-0.2888
N	-2.6679	0.2571	-0.1366
C	-4.471	-0.9816	-1.0762
C	-4.2928	1.4356	-1.4142
H	-3.2203	4.2003	-1.2556
H	-1.2021	5.5223	0.0962
H	0.6938	2.8357	2.0967
H	0.1243	4.4896	2.4711
H	1.1683	4.2138	1.0526
H	-4.9939	-1.9207	-1.2247
C	-4.9368	0.2117	-1.6425
H	-4.681	2.3612	-1.8259
H	-5.8337	0.1927	-2.2546
C	2.7466	-2.1393	0.4185
O	3.2474	-3.0054	1.0277

X

ZPE = -2250.32

Mn	-0.8585	-1.775	-0.9331
N	-1.1183	-1.3185	1.2352
N	2.1357	-2.7255	-0.3137

N	0.9385	-2.2305	1.3967
N	-3.1334	-0.5497	0.5727
N	-3.7452	-0.4334	-1.4806
C	0.8939	-2.3146	0.018
C	-2.7234	-0.8654	-0.7132
C	-1.5067	-3.4128	-0.9449
C	2.5532	-2.9376	-1.6949
H	3.5907	-2.6145	-1.8161
C	2.1817	-2.6198	1.8955
C	-0.1873	-1.7344	2.0857
C	-0.3719	-1.6834	3.4655
H	0.3841	-2.0277	4.1634
C	-1.5891	-1.151	3.9109
H	-1.7752	-1.0777	4.9783
C	-2.5758	-0.7187	3.0163
H	-3.5222	-0.3218	3.3685
C	-2.2826	-0.8474	1.6576
C	-4.3989	0.0329	0.5799
H	-4.8952	0.3561	1.4828
C	-4.7805	0.1083	-0.7167
H	-5.6821	0.5006	-1.1651
C	-3.762	-0.5481	-2.9347
H	-2.764	-0.8621	-3.2539
H	-3.9992	0.423	-3.3796
H	-4.5097	-1.2808	-3.2513
O	-1.9241	-4.5221	-1.013
H	2.4692	-3.9931	-1.9691
H	1.9023	-2.3368	-2.3384
C	2.9316	-2.935	0.8126
H	2.4233	-2.617	2.9482
H	3.957	-3.2669	0.739
O	-0.4059	-1.0722	-3.3566
C	0	-0.006	-2.7844
O	-0.0005	-0.0027	-1.458
O	0.4064	1.057	-3.3621
Mn	0.8581	1.7711	-0.9393
C	2.7233	0.8626	-0.7164
C	-0.8939	2.3145	0.0099
C	1.5055	3.4092	-0.9584
N	3.7451	0.4279	-1.4823

N	3.1336	0.5522	0.5706
N	-0.9382	2.2359	1.3889
N	-2.1356	2.7243	-0.3232
O	1.9218	4.5186	-1.0318
C	3.7618	0.537	-2.9369
C	4.7807	-0.1106	-0.7165
C	4.3993	-0.0301	0.5799
C	2.283	0.8539	1.6545
C	0.1878	1.7425	2.0795
C	-2.1812	2.6276	1.8864
C	-2.9312	2.9385	0.8024
C	-2.5532	2.9318	-1.7051
H	4.5085	1.2695	-3.2563
H	4.0004	-0.4355	-3.3779
H	2.7634	0.8484	-3.2573
H	5.6823	-0.5044	-1.1634
H	4.8958	-0.3497	1.484
N	1.1186	1.3236	1.2305
C	2.5764	0.7303	3.0136
C	0.3725	1.6965	3.4596
H	-2.4225	2.629	2.9391
H	-3.9567	3.2703	0.7276
H	-1.9022	2.3289	-2.3467
H	-2.4694	3.9863	-1.9828
H	-3.5906	2.6081	-1.8253
H	3.5228	0.3345	3.3671
C	1.5897	1.1658	3.9067
H	-0.3834	2.0434	4.1563
H	1.776	1.0964	4.9744

XI

ZPE = -1181.68

Mn	0.0202	-0.654	-0.3925
O	-0.19	-0.5639	2.5626
N	0.0088	1.3638	-0.2256
N	-3.1787	-0.8151	-0.373
N	-2.2351	1.1076	-0.2461
N	2.2488	1.1175	-0.1662

N	3.1916	-0.8036	-0.3429
C	-1.9526	-0.2476	-0.3877
C	1.9631	-0.2376	-0.3118
C	0.0497	-2.5908	-0.0769
C	-0.0669	-1.0812	1.4598
C	-3.4189	-2.2498	-0.479
H	-3.7932	-2.6408	0.471
C	-3.6023	1.3467	-0.1437
C	-1.1589	2.0044	-0.1407
C	-1.2258	3.3815	0.05
H	-2.1715	3.9077	0.1107
C	-0.0053	4.0571	0.1694
H	-0.0115	5.1322	0.3211
C	1.221	3.3869	0.1108
H	2.1609	3.9158	0.2205
C	1.1694	2.0093	-0.09
C	3.6188	1.3592	-0.1116
H	4.0451	2.3445	0.0004
C	4.207	0.1446	-0.2264
H	5.2516	-0.1309	-0.2329
C	3.4125	-2.241	-0.4743
H	3.1417	-2.578	-1.4779
H	2.8017	-2.771	0.2594
H	4.4669	-2.4535	-0.2922
O	0.0417	-2.4749	1.3677
H	-4.1504	-2.4464	-1.2664
H	-2.473	-2.734	-0.7241
C	-4.1926	0.1311	-0.2235
H	-4.0265	2.333	-0.0305
H	-5.2361	-0.1467	-0.194
O	0.0398	-3.7375	-0.5082

XII

ZPE = -1181.73

Mn	0	-0.6912	-0.0315
O	0.0003	-2.25	2.4352
N	0	1.3788	-0.0194

N	-3.1991	-0.7607	0.0484
N	-2.2479	1.1627	0.0057
N	2.2478	1.1628	0.0056
N	3.1991	-0.7607	0.0483
C	-1.9783	-0.1907	0.027
C	1.9783	-0.1907	0.027
C	0	-2.3395	-0.9992
C	-0.0001	-1.5238	1.51
C	-3.4267	-2.2017	0.0718
H	-4.1049	-2.4559	0.8895
C	-3.6175	1.414	0.0167
C	-1.1587	2.0474	-0.025
C	-1.2189	3.4369	-0.0469
H	-2.1654	3.9658	-0.0488
C	0	4.1225	-0.0613
H	0	5.2079	-0.0792
C	1.2189	3.437	-0.047
H	2.1654	3.9658	-0.0488
C	1.1587	2.0474	-0.025
C	3.6174	1.4141	0.0167
H	4.0388	2.4078	0.0111
C	4.2122	0.1973	0.0393
H	5.2577	-0.0736	0.0531
C	3.4267	-2.2016	0.0718
H	2.4634	-2.6925	0.2245
H	4.1049	-2.4558	0.8895
H	3.8575	-2.5331	-0.8764
O	0	-3.5737	-0.9863
H	-3.8574	-2.5331	-0.8764
H	-2.4634	-2.6926	0.2246
C	-4.2122	0.1973	0.0393
H	-4.0388	2.4078	0.0111
H	-5.2577	-0.0737	0.0531
O	-0.0001	-1.4813	-1.943

XIII

ZPE = -1370.11

Mn	-0.0859	0.5541	-0.1181
O	1.4032	2.0403	2.2272
N	0.6962	-1.3879	0.0833
N	3.3048	1.4173	-0.8185
N	2.8117	-0.5418	-0.1225
N	-1.4781	-1.9448	-0.2987
N	-2.912	-0.6198	-1.1869
C	2.2573	0.576	-0.7195
C	-1.6253	-0.668	-0.7993
C	-1.1439	2.1825	-0.3519
C	0.8677	1.4989	1.3697
C	3.2003	2.7688	-1.3603
H	3.5285	3.4949	-0.6126
C	4.1752	-0.3833	0.1179
C	2.0021	-1.6598	0.1515
C	2.4749	-2.9446	0.409
H	3.5362	-3.1567	0.4694
C	1.523	-3.9574	0.5427
H	1.8499	-4.9723	0.7464
C	0.1618	-3.7016	0.3495
H	-0.571	-4.4999	0.3721
C	-0.1947	-2.3849	0.0834
C	-2.6654	-2.6628	-0.3714
H	-2.766	-3.6825	-0.0324
C	-3.5679	-1.8213	-0.9306
H	-4.6092	-1.9687	-1.1762
C	-3.57	0.5374	-1.7927
H	-2.8052	1.2427	-2.1171
H	-4.2255	1.0188	-1.0622
H	-4.1537	0.2077	-2.6544
O	-2.2389	2.3539	0.4784
H	3.8156	2.8659	-2.2579
H	2.1525	2.9484	-1.6092
C	4.4819	0.8605	-0.3219
H	4.7901	-1.141	0.5796
H	5.4215	1.3936	-0.3266
O	-0.977	3.0568	-1.1977
O	-1.5836	0.5533	1.715
C	-2.4985	1.3925	1.4823
O	-3.6095	1.5129	2.0129

7. Key for Intermediates

Molecule ID	Molecular Structure	Molecule ID	Molecular Structure
I	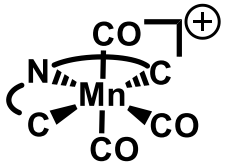	II	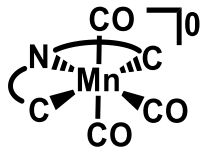
III	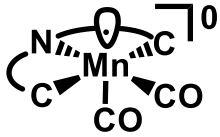	III^{+}	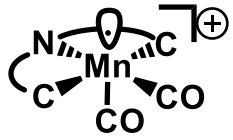
III^{2+}	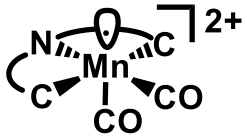	III_{dimer}	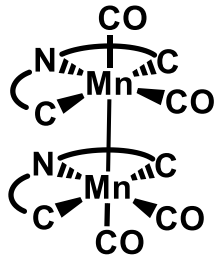
IV		IV^{+}	
V	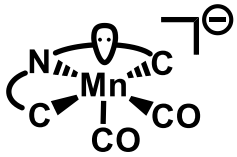	VI	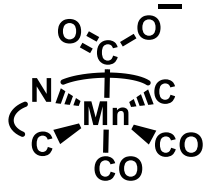
VII	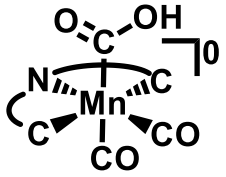	$VIII_a$	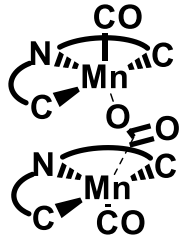
$VIII_b$	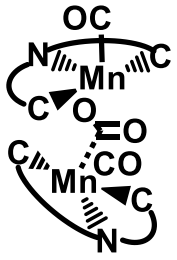	IX_a	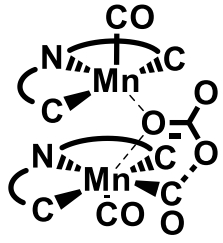

References

1. Myren, T. H. T.; Lilio, A. M.; Huntzinger, C. G.; Horstman, J. W.; Stinson, T. A.; Donadt, T. B.; Moore, C.; Lama, B.; Funke, H. H.; Luca, O. R., Manganese N-Heterocyclic Carbene Pincers for the Electrocatalytic Reduction of Carbon Dioxide. *Organometallics* **2019,** *38*, 1248-1253.
2. Vollmer, M. V.; Machan, C. W.; Clark, M. L.; Antholine, W. E.; Agarwal, J.; Schaefer, H. F., 3rd; Kubiak, C. P.; Walensky, J. R., Synthesis, Spectroscopy, and Electrochemistry of (alpha-Diimine)$M(CO)_3Br$, M = Mn, Re, Complexes: Ligands Isoelectronic to Bipyridyl Show Differences in CO_2 Reduction. *Organometallics* **2014,** *34*, 3-12.
3. Lieske, L. E.; Freeman, L. A.; Wang, G.; Dickie, D. A.; Gilliard Jr., R. J.; Machan, C. W., Metal-Free Electrochemical Reduction of Carbon Dioxide Mediated by Cyclic(Alkyl)(Amino) Carbenes. *Chemistry – A European Journal* **2019,** *25*, 6098-6101.
4. Chai, J.-D.; Head-Gordon, M., Long-range corrected hybrid density functionals with damped atom–atom dispersion corrections. *Physical Chemistry Chemical Physics* **2008,** *10*, 6615-6620.
5. Frisch, M. J.; Trucks, G. W.; Schlegel, H. B.; Scuseria, G. E.; Robb, M. A.; Cheeseman, J. R.; Scalmani, G.; Barone, V.; Petersson, G. A.; Nakatsuji, H.; Li, X.; Caricato, M.; Marenich, A. V.; Bloino, J.; Janesko, B. G.; Gomperts, R.; Mennucci, B.; Hratchian, H. P.; Ortiz, J. V.; Izmaylov, A. F.; Sonnenberg, J. L.; Williams; Ding, F.; Lipparini, F.; Egidi, F.; Goings, J.; Peng, B.; Petrone, A.; Henderson, T.; Ranasinghe, D.; Zakrzewski, V. G.; Gao, J.; Rega, N.; Zheng, G.; Liang, W.; Hada, M.; Ehara, M.; Toyota, K.; Fukuda, R.; Hasegawa, J.; Ishida, M.; Nakajima, T.; Honda, Y.; Kitao, O.; Nakai, H.; Vreven, T.; Throssell, K.; Montgomery Jr., J. A.; Peralta, J. E.; Ogliaro, F.; Bearpark, M. J.; Heyd, J. J.; Brothers, E. N.; Kudin, K. N.; Staroverov, V. N.; Keith, T. A.; Kobayashi, R.; Normand, J.; Raghavachari, K.; Rendell, A. P.; Burant, J. C.; Iyengar, S. S.; Tomasi, J.; Cossi, M.; Millam, J. M.; Klene, M.; Adamo, C.; Cammi, R.; Ochterski, J. W.; Martin, R. L.; Morokuma, K.; Farkas, O.; Foresman, J. B.; Fox, D. J. *Gaussian 16 Rev. B.01*, Wallingford, CT, 2016.
6. Andrae, D.; Häußermann, U.; Dolg, M.; Stoll, H.; Preuß, H., Energy-adjustedab initio pseudopotentials for the second and third row transition elements. *Theoretica chimica acta* **1990,** *77*, 123-141.
7. Hariharan, P. C.; Pople, J. A., The influence of polarization functions on molecular orbital hydrogenation energies. *Theoretica chimica acta* **1973,** *28*, 213-222.
8. Li, H.; Pomelli, C. S.; Jensen, J. H., Continuum solvation of large molecules described by QM/MM: a semi-iterative implementation of the PCM/EFP interface. *Theoretical Chemistry Accounts* **2003,** *109*, 71-84.
9. Li, H.; Jensen, J. H., Improving the efficiency and convergence of geometry optimization with the polarizable continuum model: New energy gradients and molecular surface tessellation. *Journal of Computational Chemistry* **2004,** *25*, 1449-1462.
10. Reed, A. E.; Weinstock, R. B.; Weinhold, F., Natural population analysis. *The Journal of Chemical Physics* **1985,** *83*, 735-746.
11. Namazian, M.; Lin, C. Y.; Coote, M. L., Benchmark Calculations of Absolute Reduction Potential of Ferricinium/Ferrocene Couple in Nonaqueous Solutions. *Journal of Chemical Theory and Computation* **2010,** *6*, 2721-2725.

12. Thapa, B.; Schlegel, H. B., Density Functional Theory Calculation of pKa's of Thiols in Aqueous Solution Using Explicit Water Molecules and the Polarizable Continuum Model. *The Journal of Physical Chemistry A* **2016,** *120*, 5726-5735.
13. Kaljurand, I.; Kütt, A.; Sooväli, L.; Rodima, T.; Mäemets, V.; Leito, I.; Koppel, I. A., Extension of the Self-Consistent Spectrophotometric Basicity Scale in Acetonitrile to a Full Span of 28 pKa Units: Unification of Different Basicity Scales. *The Journal of Organic Chemistry* **2005,** *70* , 1019-1028.
14. Zhao, Y.; Truhlar, D. G., The M06 suite of density functionals for main group thermochemistry,
thermochemical kinetics, noncovalent interactions, excited states,
and transition elements: two new functionals and systematic testing
of four M06-class functionals and 12 other functionals. *Theor Chem Account* **2008,** *120*, 215-241.